

Deanship of Graduate Studies

Al-Quds University

Radium isotopes concentration in groundwater of
Bethlehem and Hebron Districts

By

Rita Najeeb Ibrahim Elias

M.Sc. Thesis

Jerusalem- Palestine

1431/2010

Radium isotopes concentration in groundwater of
Bethlehem and Hebron Districts

Prepared By:

Rita Najeeb Ibrahim Elias

B.Sc.Biology and Biochemistry, Birzeit University

Maitrise, Biochemistry, Paris VII (Jussieu) France

Supervisor: Dr. Amer Marie

A thesis Submitted in Partial fulfillment of requirements for
the degree of Master of Science in

Environmental Studies

Department of Earth and Environmental Sciences

Faculty of Science and Technology- Al-Quds University

1431/2010

Al-Quds University
Deanship of Graduate Studies
Environmental Studies
Department of Earth and Environmental Sciences

Thesis Approval

Radium isotopes concentration in groundwater of Bethlehem-Hebron
Districts

Prepared By: Rita Najeeb Ibrahim Elias

Registration No: 20520163

Supervisor: Dr. Amer Marie

Master thesis submitted and accepted:

The names and signatures of examining Committee members are as follows:

1. Head of Committee: Dr. Amer Marie Signature.....
2. Internal Examiner: Dr. Jawad Hassan Signature.....
3. External Examiner: Dr. Saed Al-Khayat Signature.....

Jerusalem-Palestine

1431/2010

Dedication

To my beloved family: husband Elias, children Anton, Haytham, Loay and my mother in law Milia as they were my great support and strength. I will also not forget my beloved mother Margaret and my brother Joseph who were beside me all the time.

Declaration

I will certify that this thesis is submitted for the Masters degree as a result of my own research except where otherwise acknowledged. This thesis has not been submitted for a higher degree to any other university or institution.

Signature

Rita Najeeb Ibrahim Elias

Date

Acknowledgements:

I would like to express my deep thanks to the US Agency for International Development/ MERC for their financial support through their project entitled “The salinity curse of the Middle East fossil groundwater: the Radioactivity factor”. Project Number M 25_060 and Award Number TA_MOU_05_M25_060.

My deep gratitude and appreciation to my advisor Dr. Amer Marei for his full academic support. Special thanks to Mrs. Yasmin Abdel Al, Miss Manal Al Khateeb, Mr. Mahmoud Amarnah, Mr. Ala Amer and Husam Utair in the Water and Environmental Laboratory Unit at Al-Qud’s University for their help in collecting the samples and preparing the materials. A special word of appreciation is due to the Department of Earth and Environmental Sciences especially to Dr. Adnan Lahham, Dr. Qasem Abdul-Jaber, Dr. Mutaz Qutob and Mr. Mohammad Sbaih for their efforts during my study period.

I will appreciate the efforts of Mr. Mohammad Hdedoun for assisting in the information needed during the sampling campaign and Mr. Deeb Abed Al Ghafour from the PWA.

Last, but not least, I would thank the Biology Department at Bethlehem University, especially Prof. Adnan Shqueir, Prof. Moein Kanaan, Dr. Naim Iraqi, Dr. Hashem Shahin, Mr. Ghassan Handal with special thanks to Miss Mary Odeh and Mr. Nader Hazboun for their full support and opening for me the opportunity to continue my postgraduate studies. Also the efforts of Dr. Alfred Abed Rabbo and Miss Reem Zeitoun from Bethlehem University are appreciated.

Abstract

The lack of resources in the West bank and the increase in the population, led to the increase in water demand, as groundwater is considered the major source of water to the Palestinians.

The main objectives of this research are to understand the occurrence and distribution of natural radionuclides in some wells in Upper and Lower Cenomanian aquifer in the southern part of the West Bank and find correlations between Radium isotope concentrations and some of the physical and chemical characteristics of the groundwater.

The Radium isotopes (^{226}Ra and ^{222}Rn) as well as physical and chemical characteristics were measured for groundwater samples collected from different wells in Bethlehem–Hebron districts. All Radium measurements do not exceed the international standards for drinking water.

Several factors controlling the Radium concentrations had been studied. In both Upper and Lower Cenomanian Aquifer a very good positive correlation was indicated between well depth and ^{222}Rn concentration. While a negative correlation was observed between the $^{226}\text{Ra}/^{222}\text{Rn}$ ratio and the well depth in the studied wells in Bethlehem–Hebron districts.

The low concentration of ^{226}Ra (0.0055 Bq/L–0.017 Bq/L) over the ^{222}Rn concentration (2.24 Bq/L–6.75Bq/L) had lead the possibility of studying the mechanism of ^{226}Ra in the Upper Aquifer. The results had revealed a strong negative correlation between ^{226}Ra concentration and saturation indices with ($r= 0.86$). And a strong correlation between ^{226}Ra concentration and total hardness of the water with coefficient correlation ($r= 0.99$)

These results had led to the possibility of co- precipitation of ^{226}Ra with the Ca^{+2} salts in the studied wells in Bethlehem–Hebron districts in the Upper Aquifer

^{222}Rn concentration will increase with a coefficient correlation of $r=0.7$ with water direction from West to East, while no trend was observed between the ^{226}Ra concentration and water direction going from West to East. This increase in the Radon concentration could be ascribed to the increasing of faults while going from West to East in the Southern part of the Mountain Aquifer.

تركيز نظائر الراديوم المشعة في المياه الجوفية في مقاطعة بيت لحم- الخليل

ملخص

شكلت قلة مصادر المياه في الضفة الغربية وازدياد التعداد السكاني , الى زيادة طلب المياه. تعد المياه الجوفية المصدر الأساسي للفلسطينيين , فمن الضروري أن نتحقق من صلاحية المياه من الناحية الإشعاعية.

ويقوم أهمية البحث في معرفة تواجد وتوزيع النظائر المشعة للراديوم في بعض الآبار في المناطق الجنوبية للضفة الغربية و ثم إيجاد علاقات بين النظائر المشعة للراديوم والصفات الطبيعية والكيميائية للمياه الجوفية.

لقد تمت قياسات النظائر المشعة للراديوم وهي (^{226}Ra , ^{222}Rn) والصفات الطبيعية والكيميائية لبعض الآبار في منطقة بيت لحم- الخليل. أما نتائج النظائر المشعة للراديوم فهي دون المواصفات العالمية لمياه الشرب.

لقد تبين من خلال النتائج في الحوضين السفلي والعلوي أنه يوجد علاقة إيجابية بين عمق الآبار وتركيز الرادون (^{222}Rn) في الآبار. بينما يوجد علاقة سلبية بين عمق الآبار والنسبة $^{226}\text{Ra}/^{222}\text{Rn}$ إن التركيز المنخفض للراديوم في الحوض العلوي ^{226}Ra (0.0055–0.017Bq/L) على التركيز العالي للرادون (2.24Bq/L_ 6.75Bq/L) أدى الى احتمالية دراسة آلية تصرف الراديوم في مياه الحوض العلوي. لقد أظهرت النتائج علاقة سلبية قوية بين تركيز الراديوم و saturation indices بمعامل ارتباط ($r=0.86$) و علاقة سلبية قوية بين تركيز الراديوم و total hardness بمعامل

إرتباط ($r= 0.99$). لقد أدت هذه النتائج إلى إحتمالية ترسيب الراديوم (^{226}Ra) مع الكالسيوم في الحوض العلوي.

تبين أيضا أن الرادون يزداد بمعامل إرتباط ($r=0.7$) عن توجه المياه من جبال الخليل غربا باتجاه الشرق بينما لا يوجد علاقة بين الراديوم وتوجه المياه شرقاً, ربما يعود ذلك الى تزايد الصدوع كلما اتجهنا شرقاً في المنطقة الجنوبية للحوض الجبلي (Mountain Aquifer).

Table of Contents	Page
Dedication	i
Declaration	ii
Acknowledgements	iii
English Abstract	iv
Arabic Abstract	vi
Table of Contents	viii
List of Tables	xiv
List of Figures	xv
Definition	xviii
Abbreviation	xx
Chapter One : Preface	1
1.1 Introduction	1
1.2 Importance of the research	3
1.3 Objectives of the research	4
1.4 Hypothesis	4
Chapter Two: Study area	6
2.1 Introduction	6

2.2	Groundwater Basins	7
2.2.1	Western Groundwater Basin	8
2.2.2	Northeastern Groundwater Basin	8
2.2.2	Eastern Groundwater Basin	8
2.3	Geological setting	10
2.3.1	Lithology	10
2.3.1.1	Lower Beit Kahil Formation (Lower Cenomanian)	15
2.3.1.2	Upper Beit Kahil Formation (Lower Cenomanian)	15
2.3.1.3	Yatta Formation (Lower Cenomanian)	15
2.3.1.4	Hebron Formation (Upper Cenomanian)	15
2.3.1.5	Bethlehem Formation (Upper Cenomanian)	16
2.3.1.6	Jerusalem Formation (Turonian)	16
2.3.2	Diagenesis of carbonate rocks	16
	Chapter Three: Radioactivity in the Environment	17
3.1	Introduction	17
3.2	Radioactive decay	21
3.3	Types of Environmental Radioactivity	23
3.3.1	Sources of Natural Radiation Exposures	25

3.3.1.1 Cosmogenic Radionuclides	25
3.3.1.2 Primordial nuclides	26
3.3.2 Sources of Artificial Radioactivity–Anthropogenic Radionuclides	26
3.4 Radium in groundwater	27
3.4.1 Geological Factor	27
3.4.2 Chemical Factor	28
3.4.3 Physical Factor	30
3.5 Units of measurements for Radium elements in water	32
3.6 Maximum permissible Concentrations of Radium elements in water	32
3.7 Radioactive elements impact on human health	33
Chapter Four: Literature Review	34
Chapter Five: Methodology	40
5.1 Sampling sites	40
5.2 Sampling procedure	42
5.2.1 Chemical sampling procedure	42
5.2.2 Radium isotopes sampling procedure	42
5.2.3 Radon sampling procedure	43

5.3	Measurements	44
5.3.1	Chemical analysis of water	44
5.3.2	Radium isotopes analysis	44
5.3.3	Radon analysis	45
5.3	Calculations	47
Chapter Six: Results and Discussion		49
6.1	Results	49
6.2	Water type classification	52
6.2.1	Piper diagram	52
6.3	Saturation Indices	55
6.4	Radium isotopes analysis in the Upper and Lower Cenomanian Aquifers	57
6.4.1	Upper Cenomanian–Turonian Aquifer	58
6.4.1.1	Upper Cenomanian Aquifer–Well depth and Electrical Conductivity (EC)	58
6.4.1.2	Upper Cenomanian Aquifer–Well depth and sulphate concentration (SO ₄ ²⁻)	59
6.4.1.3	Upper Cenomanian Aquifer–Well depth and nitrate concentration (NO ₃ ⁻)	60
6.4.1.4	Upper Cenomanian Aquifer–Well depth and Radon	61

concentration (^{222}Rn)	
6.4.1.5 Upper Cenomanian Aquifer–Well depth and $^{226}\text{Ra}/^{222}\text{Rn}$ ratio	62
6.4.1.6 Upper Cenomanian Aquifer–Saturation Index (calcite) with ^{226}Ra concentration	63
6.4.2 Middle Cenomanian Aquiclude	65
6.4.3 Lower Cenomanian Aquifer	65
6.4.3.1 Lower Cenomanian Aquifer–Well depth and Electrical Conductivity (EC)	66
6.4.3.2 Lower Cenomanian Aquifer–Well depth and Radon concentration (^{222}Rn)	67
6.4.3.3 Lower Cenomanian Aquifer–Well depth and $^{226}\text{Ra}/^{222}\text{Rn}$ ratio	67
6.4.4 Data Interpretation for Upper and Lower Cenomanian Aquifers	68
6.4.4.1 Well depth and ^{222}Rn concentration in Upper and Lower Aquifers	68
6.4.4.2 Correlation between ^{222}Rn , ^{226}Ra concentration and distance from West and East	69
6.5 Summary of the results	72
6.6 Conclusions	73
6.7 Recommendations	74
References	75
Appendix	81

List of Tables:

Table No.	Table title	Page
Table 2.1	Generalized stratigraphic column of the West Bank	14
Table 5.1	Sampling sites in Bethlehem and Hebron districts	40
Table 6.1	Results of physical and Radium isotopes measurements	50
Table 6.2	Results of the chemical analysis in mg/L	51
Table 6.3	Saturation Indices of the water of the wells studied in Bethlehem–Hebron districts, with respect to calcite, dolomite and gypsum minerals	56
Table 6.4	Radium, Radon concentration, Total Hardness and well depth of the study area.	57

List of Figures:

Figure No.	Figure title	Page
Figure 2.1	Location map of the West Bank	6
Figure 2.2	Map showing the three Basins in the West Bank	10
Figure 2.3	Hydrogeological cross section from West to East of the West Bank	11
Figure 2.4	NW_SE hydrological cross section showing the regional aquifers and aquicludes through the Mountain Aquifer	12
Figure 2.5	General geological and structural map of the West Bank	13
Figure 3.1	Natural Decay Series: Uranium–238	18
Figure 3.2	Natural Decay Series: Uranium–235	19
Figure 3.3	Natural Decay Series: Thorium–232	20
Figure 3.4	Pie chart showing the relative contributions from natural and man– made sources of radiation worldwide	24
Figure 3.5	The recoil process of Radon in groundwater	30
Figure 3.6.a	Schematic diagram of nanoporosity in solids found in aquifers	31
Figure 3.6.b	Schematic diagram of Radon and other U-Th series isotope enter the nanopores by recoil	31
Figure 5.1	Location of the wells in Bethlehem_Hebron districts in the West Bank	41

Figure 5.2	Technical circuit of the sample filtration used for Radium preconcentration	43
Figure 5.3	Close loop during ^{226}Ra measurements at Al Qud's University	45
Figure 5.4	Radon measurement using RAD7- H_2O	46
Figure 6.1	Piper trilinear diagram with classification of water types	53
Figure 6.2	Piper diagram showing the wells studied in Bethlehem–Hebron districts	54
Figure 6.3	Negative Linear correlation between well depth and Electrical Conductivity in the Upper Aquifer	59
Figure 6.4	Negative Linear correlation between well depth and sulphate concentration in the Upper Aquifer	60
Figure 6.5	Negative Linear correlations between well depth and nitrate concentration in the Upper Aquifer	61
Figure 6.6	Positive Linear correlation between well depth and ^{222}Rn concentration in the Upper Aquifer	62
Figure 6.7	Negative Linear correlation between well depth and $^{226}\text{Ra}/^{222}\text{Rn}$ ratio in the Upper Aquifer	63
Figure 6.8	Negative Linear correlation between Saturation Indices (calcite) and ^{226}Ra concentration in the Upper Aquifer	64
Figure 6.9	Negative Linear correlation between Total Hardness(mg/L CaCO_3) and ^{226}Ra concentration in the Upper Aquifer	65
Figure 6.10	Negative Linear correlation between well depth and Electrical Conductivity in the Lower Aquifer	66
Figure 6.11	Positive Linear correlation between well depth and ^{222}Rn – concentration in the Lower Aquifer	67
Figure 6.12	Negative Linear correlation between well depth and $^{226}\text{Ra}/^{222}\text{Rn}$ ratio in the Lower Aquifer	68

Figure 6.13	Positive Linear correlation between well depth and ^{222}Rn concentration of the Upper Aquifer red circle and the Lower Aquifer blue circle	69
Figure 6.14:	Positive Linear correlation between the distance to the East and ^{222}Rn concentration	70
Figure 6.15:	Positive Linear correlation between the distance to the East and ^{226}Ra concentration	70
Figure 6.16:	Location of the studied wells in relation to the ^{222}Rn concentration and the faults from West to East in Bethlehem_Hebron districts	71

Definitions:

Activity: The decay rate of a radioactive material, generally expressed as the number of disintegration per unit time.

Alpha particle: consist of two protons and two neutrons bound together into a particle identical to a helium nucleus, that is ${}_2^4\text{He}^{2+}$ or He^{2+}

Beta particle: is a high speed electron (e^-) emitted as a result of the conversion of a neutron to a proton in a nuclei undergoing radioactive decay.

Diagenesis: The physical and chemical changes occurring during the conversion of sediment to sedimentary rock.

Ionic Strength: The ionic strength of the solution is a measure of the concentration of ions in that solution ($I = \frac{1}{2} \sum c_i z_i^2$ where c_i = the molar concentration of the ion i , z_i = the charge number of that ion i).

Isotopes: are atoms with different numbers of neutrons in their nuclei. Isotopes of an element have nuclei with the same number of protons (same atomic number) but different numbers of neutrons (different mass number).

Porosity: is the amount of water that can be stored in an aquifer is equal to the volume between the soil grains. Porosity = volume of voids/ Total volume

Radioactive decay: is the process in which an unstable atomic nucleus loses energy

by emitting ionizing particles and radiation.

Radioactive nuclides (radionuclides): unstable nuclides that tend to change spontaneously to other species of nuclides through various decay reactions.

Radioactivity: refers to the particles (α , β particles or δ rays) which are emitted from nuclei as a result of nuclear instability.

Secular equilibrium: is a situation in which the quantity of a radioactive isotope remains constant because its production rate is equal to its decay rate.

Abbreviations:

eV : Electron Volt

Gy : Gray

J/ Kg: Joule / kilogram

K_d: Adsorption coefficient

KeV: Kilo electron volt

L : liter

m : meters

Chapter One

Introduction

1.1 Introduction

The increase demand of water due to the rise in population and the lack of resources in the West Bank, had led to investigate the quality of groundwater including the radioactive elements. Naturally occurring radioactive elements are found in water, soils and rocks. Uranium and Thorium, the common long-lived radioactive elements, decay slowly to produce other radioactive elements which in turn undergo radioactive decay. ^{238}U will decay producing ^{226}Ra and ^{222}Rn as its progeny; ^{235}U will produce ^{223}Ra and ^{219}Rn while ^{232}Th will produce ^{228}Ra , ^{224}Ra and ^{220}Rn as its progeny. These radioactive elements can have serious effect on flora, fauna and have acute health effects on human beings when they exceed the permissible levels set by the local or international authorities.

The Palestinian population is 2,350,583 lived in the West Bank (PCBS, 2007) in an area about 5860 km². As the Palestinians are denied to share water from the Jordan River, water resources in the West bank are restricted mainly to groundwater that are abstracted from the wells and springs and water purchased from Israeli Water Company (Mekorot). The quantity of water pumped from the wells in the West Bank reaches 57.76 million m³ in 2005 for domestic and agricultural use (PCBS Press Release, 2007). According to Water Authority data, the water quantity purchased from Israeli Water Company (Mekorot) is about 40 million m³ in the West Bank in 2006 (PCBS Press Release, 2007). The highest quantity of water purchased was in August and reached 4.2 million m³ and the lowest was in February with 2.4 million m³ (PCBS Press Release, 2007). Groundwater is considered to be the major source in the West Bank; the overexploitation of groundwater aquifer had led

to the degradation of groundwater quality and affects the sustainability of the resources in the future. The major issue is that water resources are very limited and they do not meet the needs of the existing population and even more for the coming generations. Based on multi-model predictions, the Intergovernmental Panel on Climate change report predicts a significant reduction in precipitation in the Middle East during the next decades, which will likely exacerbate the water crisis in the region (Vengosh, et al., 2008).

The West Bank overlies three groundwater basins that are connected together and is known as the Mountain Aquifer Basin: the Eastern Aquifer Basin, The Western Aquifer Basin and the Northeastern Aquifer Basin. In the Eastern Aquifer Basin, Palestinians pump 26.1 million m³/yr from 203 wells; 154 wells are for agricultural use, 33 wells are abandoned, 10 wells are for domestic use and 6 wells are under the West Bank Water Department. The Western Aquifer Basin is the largest of all groundwater basins in Historical Palestine, where there are 155 wells with an average pumping rate of 22 million m³/yr. 126 wells are for agricultural use, 8 wells are abandoned, 17 wells are for domestic use and 4 wells are under the West Bank Water Department. The Northeastern Aquifer Basin is the smallest of the three basins and by that has the smallest portion of recharge as well. Palestinians pumps 14.5 million m³/yr from 143 wells. 76 wells are for agricultural use, 54 wells are abandoned and 9 wells are for domestic use while 4 wells are under the West Bank Water Department (PWA, 2004).

The quantity of supplied water for domestic use per capita is 96.8 liter/capita/day in the West Bank, while the World Health Organization recommend 100 liters of water per person per day as the minimum quantity for basic consumption (PCBS Press Release, 2007).

1.2 Importance of the research

This research aims to investigate the radioactivity concentrations in the groundwater aquifers, a new topic that has not been studied in the West Bank. This research is the first in the West Bank in measuring the Radium isotopes in groundwater. We are going to emphasize on the Radium isotopes tracing applications such as the origin of these radioactive elements in groundwater and the rate of their water rock interaction as well as their transport in the aquifer itself. This study will provide a mapping of radioactivity in groundwater in the southern part of the West Bank. So together with the hydrogeology and geochemistry investigations will facilitate the prediction of specific areas with high Radium concentrations.

The importance of this study is to illustrate the distribution and behavior of Radium isotopes that is found in the groundwater in the southern part of the West Bank. The most radiotoxic and the most important radionuclides in the radioactive decay chain is Radium, which is defined as a Group A carcinogen. Epidemiological studies had related bone cancer (osteosarcoma) with the consumption of groundwater having high radium activities > 0.185 Bq/L (combined concentration of ^{228}Ra and ^{226}Ra). The Environmental Protection Agency and the European Community have a strict drinking water limit of 0.5 Bq/L for ^{226}Ra and 0.2 Bq/L for ^{228}Ra while the upper limit of the short lived ^{224}Ra is 2 Bq/L (EPA, 2000).

The practical importance derives from the human health risks associated with the ingestion of Radium and the inhalation of Radon and its daughter products. While the scientific importance derives largely from the potential applications of Radium isotopes in tracing the mechanisms and rates of water-rock interaction and element transport in aquifers. The information from such scientific studies can lead to an improved understanding of the

factors controlling water quality and can be useful in establishing better strategies for the use and protection of underground water resources (Sturchio et al., 2001).

1.3 Objectives of the research

The main objective on which this study is based is that water resources tested are safe to use when it comes to their radium isotopes concentration. Accordingly this research aims to investigate the radium isotopes concentration in groundwater aquifers, a topic that has not been studied before in detail. This will provide a step forward towards the comprehensive mapping of radioactivity in groundwater.

The major objective of this study is to understand the occurrence and distribution of Radium isotopes in groundwater at the upper Cenomanian-Turonian aquifer and at the lower Cenomanian aquifer that are part of the Mountain aquifer in the Southern part of the West Bank. The main objectives are:

- To grasp the main concepts related to radioactivity in addition to its measurement and its natural sources.
- Measure the radioactivity in some selected wells in the southern part of the West Bank.
- Measure some of the physical and chemical characteristics of the groundwater and try to establish possible correlations between Radium and other dissolved constituents.

1.4 Hypothesis

To measure the radioactivity concentration (^{226}Ra , ^{222}Rn) in the Lower and Upper Cenomanian Aquifer and correlate the ^{226}Ra and ^{222}Rn concentration with some physical and chemical characteristics. The interpretation of the results of ^{226}Ra and ^{222}Rn concentrations and their ratios in water may lead to certain mechanisms for ^{226}Ra and ^{222}Rn

in water. In order to confirm these mechanisms certain measurements and calculations were done.

Chapter Two

Study area

2.1 Introduction

West Bank is an area of 5860 km², located 130 km from north to south, 40 km and 65 km from east to west. On the Palestinian grid, West Bank lies between 85 and 220 North and between 140 and 200 East as shown in Figure 2.1.

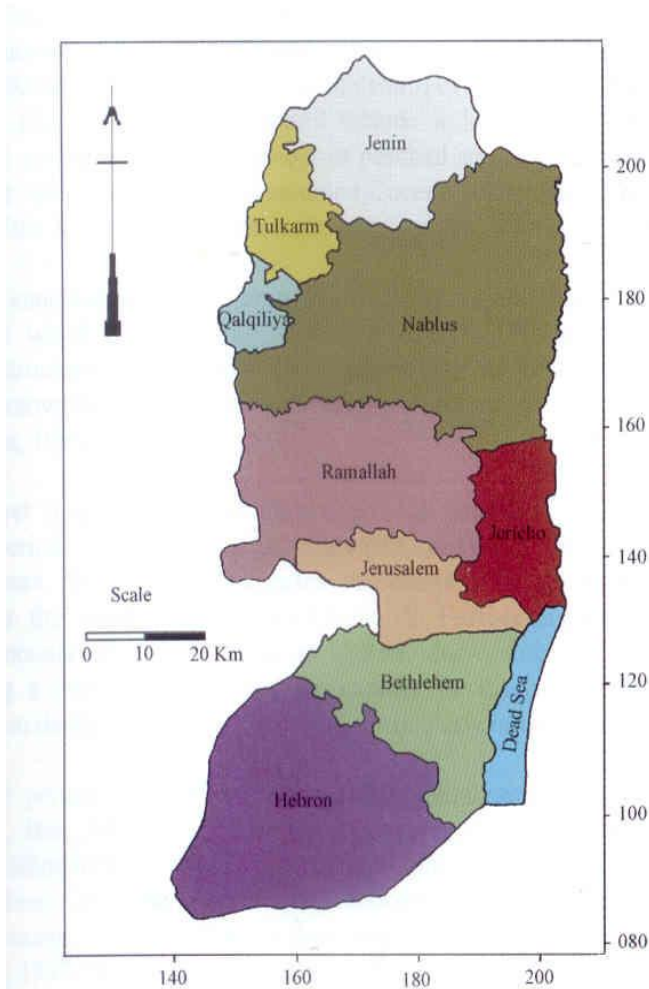


Figure 2.1: Location map of the West Bank (Qasem Abdul-Jaber et al., 1999)

The climate in the West Bank is within the Mediterranean climatic zone except for the Jordan Valley arid to semi-arid with hot summers and warm winters. The temperature

increases from north to south contrary to altitude. August is the hottest month, while January is the coldest. The mean annual temperature ranges from 22°C to 25°C. In the West Bank, rain starts in the middle of October till the end of April.

2.2 Groundwater Basins

The two major water sources available in the West Bank are the Jordan River and the West Bank Aquifer System. Palestinians are not allowed to use more than 15% of their groundwater and are denied access to Jordan River (MEnA, 1998).

The structure of the Mountain Aquifer is not a simple anticline. Rather it is a complex anticlinorium with folds plunging in various directions, affecting groundwater flow. The apex of the main anticlinal structure separates groundwater flow westwards towards the Mediterranean drainage systems or eastwards to the Jordan Valley and the Dead Sea. The main recharge area is to the windward side of the highest elevations of the mountains. The upper parts of the Yatta Formation separate an unconfined upper sub-aquifer from a lower confined sub-aquifer (Scarpa, 2002). Recharge water enters both sub-aquifers within the area of recharge. In Palestine the West Bank Aquifer system (Mountain Aquifer) extends below the area of the West Bank and it is recharged by rainfall from the mountains of the West Bank forming the phreatic portion, while the main storage areas are in the confined portions which either flows to the West towards the Israeli underground and the Mediterranean or to the East towards the Jordan Valley and the Dead Sea.. So rainfall infiltrates to the water table forming the West Bank Aquifer System which is composed of dolomite and limestone rocks of the lower Cenomanian and Turonian ages. The West Bank Aquifer System is divided into three groundwater basins as shown in Figure 2.2. And the total annual capacity of the ground aquifers is estimated at 600-650 million m³/yr (MEnA, 1998).

2.2.1 Western Groundwater Basin

The Western Basin is the largest of all groundwater basins in Palestine and is considered as one of the main aquifers. The groundwater movement in this basin is westwards towards the coastal plain in the west. The storage capacity of this basin is about 360 million m³/yr (MEnA, 1998). Eighty percent of the recharge area of this basin is located within the West Bank while 80% of the storage area is located within the Israeli borders so it is a shared basin between Palestine and Israel. Total area of this basin is 2500 km².

2.2.2 Northeastern Groundwater Basin

The Northeastern Basin consists of the Nablus-Jenin basin, is located in the large syncline of the north central part of the Samaria Mountains. It is the smallest of the three basins. The storage capacity of this basin is approximately 140 million m³/yr (MEnA, 1998). The groundwater in this basin flows north and northeast towards Bisan natural springs. Total area of this basin is 700 km².

2.2.3 Eastern Groundwater Basin

The Eastern Aquifer extends from the crest of the West Bank Mountains on the West to the Jordan River and the Dead Sea on the East. The recharge and discharge areas of this basin are completely located within the West Bank boundary. The recharge of the Eastern Groundwater Basin occurs in the outcrop regions in the mountains where most of the rain falls predominantly in the mountain outcrop regions of the Albian-Turonian formations. Some Palestinian and Israeli hydro-geologists are sub-dividing the Eastern Basin into three smaller sub-basins which are: Eastern Aquifer Sub-Basin, The Jordan Valley Floor Aquifer Sub-Basin and the Dead Sea Aquifer Sub-Basin. The Eastern Basin drain from Neogene, Pleistocene, Lower and Upper Cenomanian sub-aquifers. The Cenomanian-Turonian

aquifer system in the eastern basin can be divided into two sub units: Upper Cenomanian-Turonian sub aquifer which is thin and shallow aquifer and the Lower Cenomanian aquifer which is deep aquifer. According to the surface and subsurface hydrological divisions of the West Bank, Marsaba-Feshcha area are part of the Jerusalem Desert; accordingly it is related to the Dead Sea Aquifer Sub-Basin which is part of the Eastern Groundwater basin. The recharge area of this basin encounter over 2200 km² and the storage area over 2000 km² (Gvirtzman, 1994). The Eastern aquifer storage capacity was estimated to be about 202 milliom m³/yr (Gvirtzman, 1994).

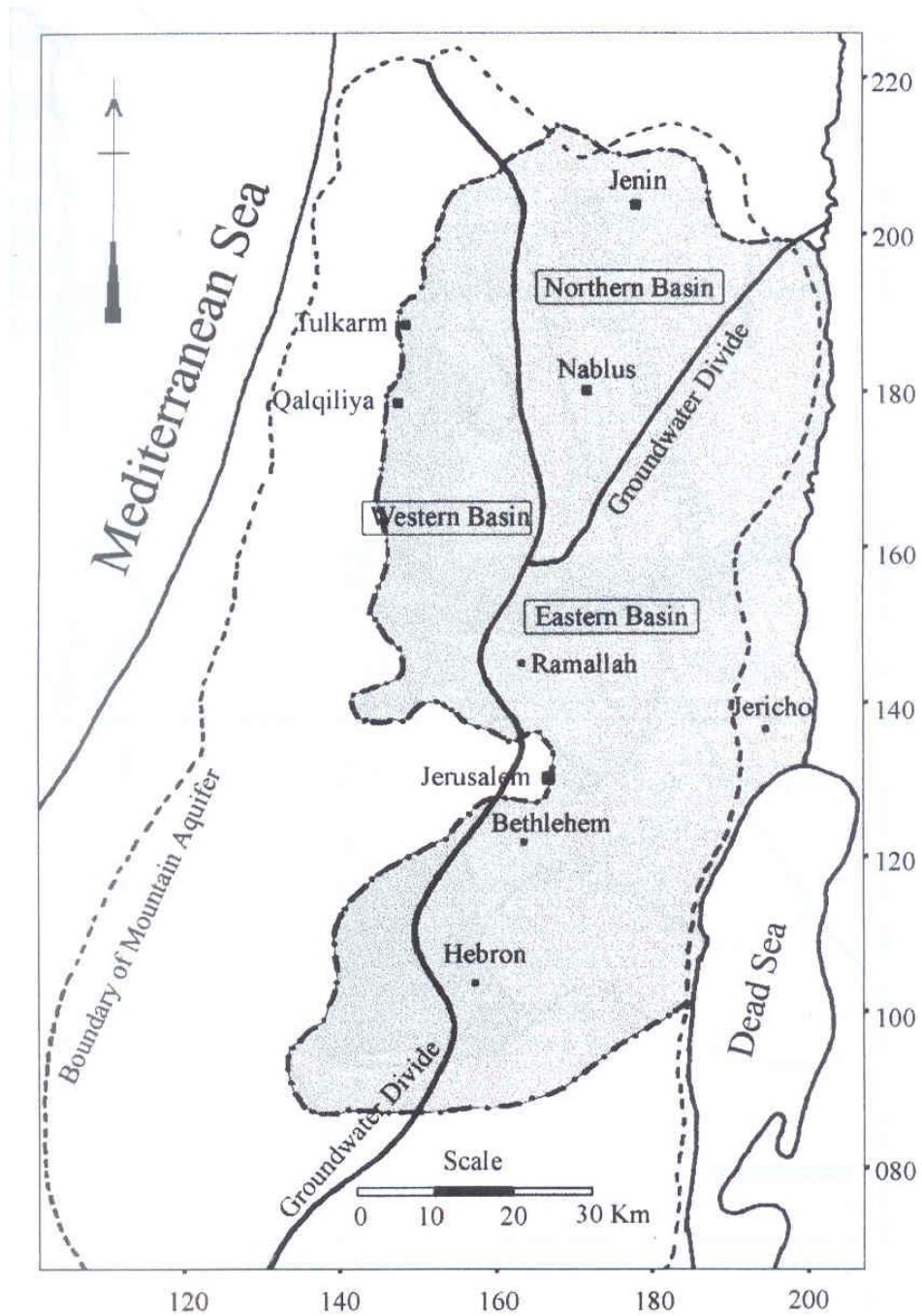


Figure 2.2: Map showing the three Basins in the West Bank (Roffe and Raffety, 1963).

2.3 Geological Setting

2.3.1 Lithology

The outcrops within the West Bank are predominantly carbonate sediments and rocks of Tertiary and Cretaceous age (Roffe and Raffety, 1965). The oldest exposed rocks belong to the Albian covered by younger strata of the Cenomanian, Turonian and Eocene, exposed

on both flanks of the anticlinal axis of the West Bank (Rofe and Raffety, 1965). Almost all exposed rocks in the West Bank extended from the lower Cretaceous to Quaternary with limited exposures of Jurassic rocks. In the Cenomanian-Turonian era, the area was dominated by thick strata of limestone and dolomite and the majority of the exposed rocks in the southern part of the West Bank are composed from limestone and dolomite. While in the Jordan Valley and the shorelines of the Dead Sea, the youngest formations of the Pleistocene-Holocene age are found. In Figures 2.3 and 2.4 shows the hydrogeological cross section from west to east of the West Bank while Figure 2.5 shows the geological map of the West Bank.

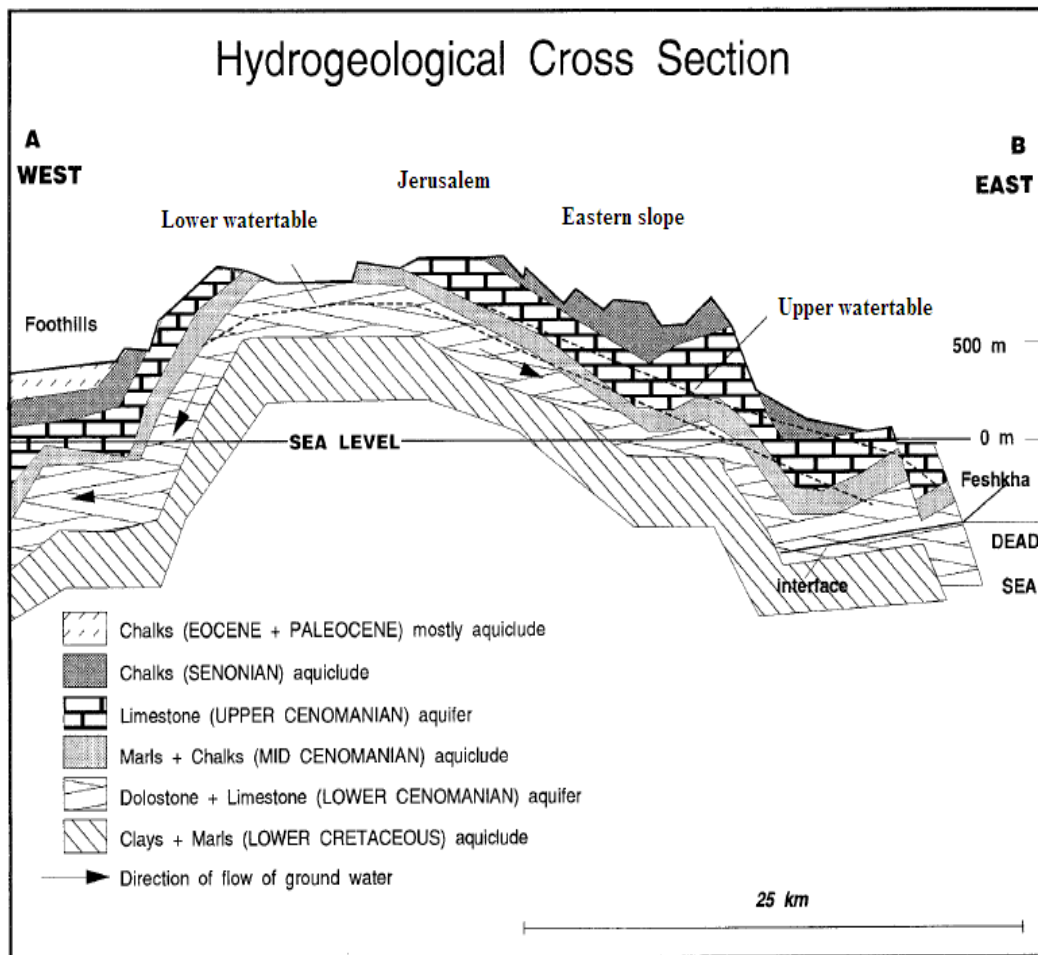


Figure 2.3: Hydrogeological cross section from West to East of the West Bank (modified after Issar, 1993).

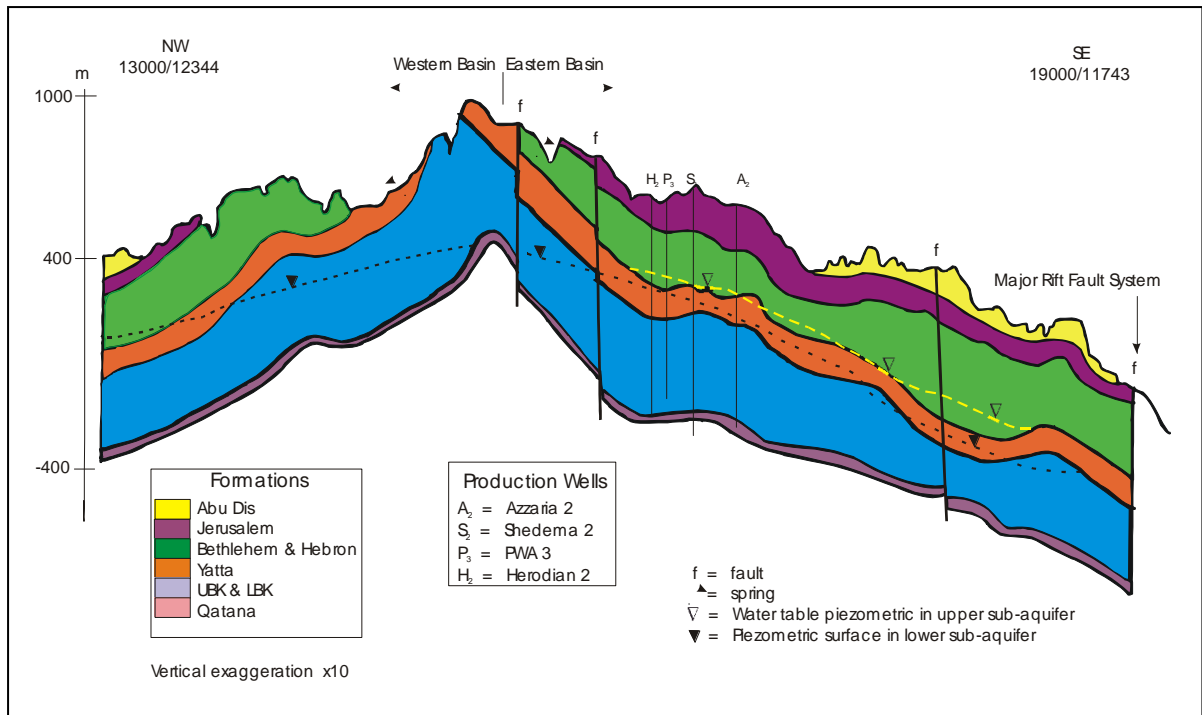


Figure 2.4: NW-SE hydrological cross section showing the regional aquifers and aquicludes through the Mountain Aquifer (After: CH2MHill, 2000)

The two main regional aquifers in the West bank are built up from Tertiary and Cretaceous rocks and these rocks are mainly made of limestone, dolomite, chalk and marl: the Upper Cenomanian Turonian aquifer composed of Jerusalem Bethlehem and Hebron Formations while the Lower Cenomanian aquifer composed of Upper and Lower Beit Kahil Formations. Yatta Formation which separate the two aquifers composed of marls and clays represents the main aquiclude in the West bank. Table (2.1) describe and illustrate the general stratigraphy of the West Bank with the Palestinian and Israeli names of the different geological formations as well as their thickness, lithology and hydrostatigric.

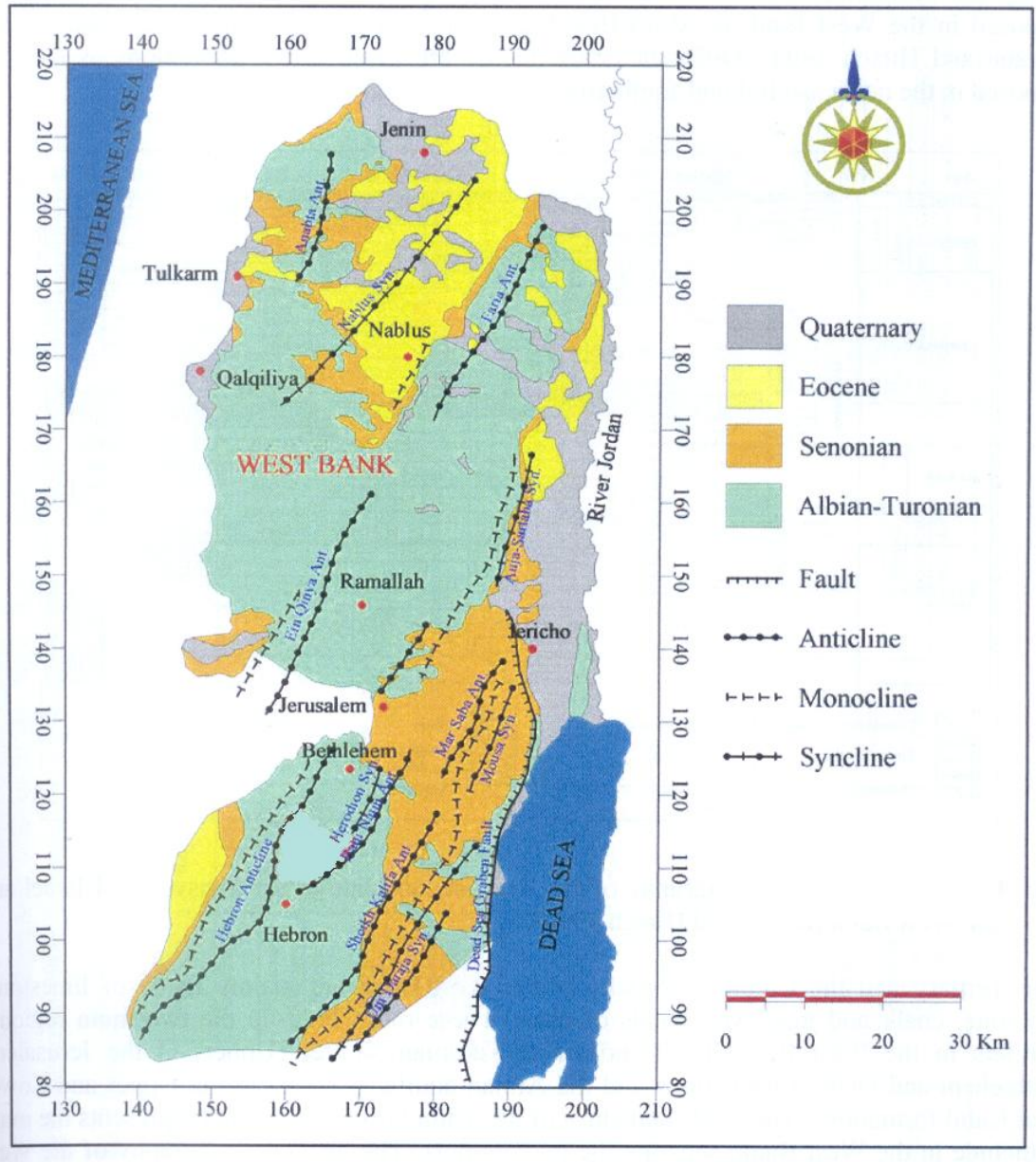


Figure 2.5: General geological and structural map of the West Bank (modified after Guttman and Zuckerman 1995).

Table 2.1: Generalized stratigraphic column of the West Bank (Guttman and Zuckerman, 1995).

Geological Time Scale			Group			Formation		Lithology	Thickness (m)	Hydrostratigraphy			
Era	System	Epoch	Palestinian		Israeli	Palestinian	Israeli						
Cenozoic	Quaternary	Holocene	Recent		Kurkar	Alluvium	Alluvium	Marl, alluvium, gravel	Variable	Aquifer			
						Gravel	River gravel			Aquifer			
		Pleistocene	Lisan		Dead Sea	Lisan	Lisan	Thinly laminated marl with gypsum bands	200+				
	Tertiary	Neogene	Pliocene-Miocene	Beida	Jenin Sub Series	Saqia	Beida	Bit Nir and Ziglag	conglomerate	0-200	Aquifer		
				Belqa		Avidat	Reef nummulitic limestone	Zor'a			Reef limestone, bedded limestone, chalk with limestone undifferentiated	Aquifer in limestone and aquiclude in chalk	
		Paleogene	Eocene			Mount Scopus	Nummulitic limestone	Taqiya	Marl, chalk and clay		Aquiclude		
							Khan Al Ahmar and Zerqa	Ghareb	Yellowish chalk		Aquiclude		
	Mesozoic	Senonian	Mastrichtian				Amman and Abu Dis	Mishash	Chalk with black chert		Aquiclude		
							Campanian	Menuha	Chalk		Aquiclude		
												Santonian	
Cretaceous			Turonian	Ajlun		Judea	Jerusalem	Bina	Limestone and dolomite (karstic)	90-120	Aquifer		
							Cenomanian	Bethlehem	Weradim	Hard gray porous dolomite	90-100	Aquifer	
								Kfar Shaul	Chalky limestone, chalk and marl	30-40	Aquitard		
			Albian						Hebron	Aminadav	Karstic limestone and dolomite	110-140	Aquifer
									Yatta	Moza	Marl, clay and marly limestone	10-20	Aquiclude
										Beit Meir	Limestone, chalky limestone and dolomite	120-140	Aquifer
			Aptian						Kurnub	Kurnub	Upper Beit Kahil	Kesalon	Limestone inter-bedded with marl
Lower Beit Kahil	Soreq	Dolomite inter-bedded with marl		110-170	Aquifer								
	Giva't Yearim	Limestone, dolomite		20-70	Aquifer								
Kefira	Limestone, dolomite and marly limestone	120-180		Aquifer									
Kurnub					Kobar	Qatana	Marl and clay	50	Aquitard				
						Ein Qinyia	Marl and marly limestone	60-70	Aquitard				
						Tammun	Clay and marl	80-150	Aquitard				
						Ein Al Asad	Limestone		Aquifer				
Nabi Said	Limestone	Aquifer											

So as we realized that Ajlun group (Judea group) belongs to the Upper Cretaceous Rocks which are divided to the following formations: (Rofe and Raffety, 1963-1965)

2.3.1.1 Lower Beit Kahil Formation (Lower Cenomanian)

The Lower Beit Kahil Formation is considered as the lowest part of the Lower Cenomanian. It consists of limestone, dolomite and marly limestone; it is considered to be a moderate to good aquifer due to the well jointed dolomitic limestone formation. Its vertical thickness ranges between 137 m in PWA1. The total thickness of this formation is nearly 160-290 m. (Rofe and Raffety, 1963-1965).

2.3.1.2 Upper Beit Kahil Formation (Lower Cenomanian)

The Upper Beit Kahil Formation represents as the upper part of the Lower Cenomanian. This formation consists of limestone and dolomite inter-bedded with marl. This formation is characterized by marl and marly limestone, as well as limestone and chalky limestone. The total thickness is of 110-250 m. (Rofe and Raffety, 1963-1965).

2.3.1.3 Yatta Formation (Middle Cenomanian)

The lower Cenomanian Yatta Formation is composed of limestone, chalky limestone, dolomite, marl and greenish clay at the bottom. Yatta Formation separates the Upper Cenomanian aquifer from the Lower Cenomanian aquifer and act as an aquiclude. Yatta Formation is 86 m thick in Herodion well 4 and 128 m in Herodion well 3 (Rofe and Raffety, 1963- 1965).

2.3.1.4 Hebron Formation (Upper Cenomanian)

The Lower Cenomanian Hebron Formation consists of the following lithology: dolomitic limestone at the top, dolomite and chalky limestone in the middle while dolomitic limestone and hard dolomite at the base. Its vertical thickness ranges between 70 m in Herodion well 4 and 120 m in PWA1 well (Rofe and Raffety, 1963-1965).

2.3.1.5 Bethlehem Formation (Upper Cenomanian)

The Upper Cenomanian Bethlehem Formation is composed of hard dolomite in its upper part, while chalk, limestone and dolomite in its lower part. Bethlehem Formation is considered to be a good aquifer due to the well-developed joints and fractures in the uppermost limestone. Its thickness ranges from 30-150 m. Its vertical thickness ranges between 88 m in PWA1 and 260 m in Herodion well 4 (Rofe and Raffety, 1963-1965).

2.3.1.6 Jerusalem Formation (Turonian)

Jerusalem Formation is from the Turonian age. It is characterized by chalky and dolomitic limestone. Due to fractures and joints of this formation turns out to be a good aquifer. Its thickness ranges between 50-140 m. The Jerusalem Formation has a thickness of about 90-100 m as in Herodion wells 3 and 4 (Rofe and Raffety, 1963-1965).

2.3.2 Diagenesis of carbonate rocks

Carbonate rocks are a class of sedimentary rocks composed primarily of carbonate minerals. The two major types of carbonate minerals are limestone and dolomite, which composed of calcite (CaCO_3) and dolomite ($\text{CaMg}(\text{CO}_3)_2$) minerals respectively. Calcite minerals can be either dissolved by groundwater or precipitated depending on several factors including the water temperature, pH, and dissolved ion concentrations. Calcite exhibits what called the retrograde solubility in which it becomes less soluble in water as the temperature increases. Whenever good conditions for precipitation occurs, calcite forms mineral coatings that cement the existing rock grains together or it can fill fractures. Karst topography and caves develop in carbonate rocks due to their solubility in dilute acidic groundwater. Cooling groundwater or mixing of different groundwater will also create conditions suitable for cave formation.

Chapter Three

Radioactivity in the Environment

3.1 Introduction

Man is exposed to both external and internal radiation. It is just recently that artificial sources of radiation have become available, while human being has been exposed to natural sources of radiation from the beginning of the universe. Natural sources of radioactivity are made up of radionuclides emitted by cosmic and earth radiations. In water the radioactivity is due to dissolved elements from these natural sources (Grainger, 1986).

Ionizing radiation produces detrimental biological effects, many studies had been progressed determining the sources and levels of radiation to which the human population is exposed, and have estimated the corresponding biological effects. The natural ionizing radiation, to which all people are exposed, includes cosmic rays and products of the decay of radioactive elements in the earth's crust and atmosphere. Part of the terrestrial radiation dose is from sources external to the body, and part is due to the inhalation and ingestion of radioactive elements in air, food and water (Degrémont, 1991).

In nature there are three radioactive decay chains. Uranium-238 (^{238}U) nucleus passes through a series of 14 transformations to become at the end stable lead-206 (^{206}Pb). Uranium-235 (^{235}U) nucleus passes through 11 transformations to become at the end stable lead-207 (^{207}Pb) while Thorium-232 (^{232}Th) nucleus passes through 11 transformations to become at the end stable lead-208 (^{208}Pb). In between these transformations exist a series of nuclides with different half lives ranging from microseconds to hundreds of thousands of years. These transformations occur by emitting alpha particles, beta particles or gamma rays. The three naturally occurring radioactive series are illustrated in Figures 1 through 3.

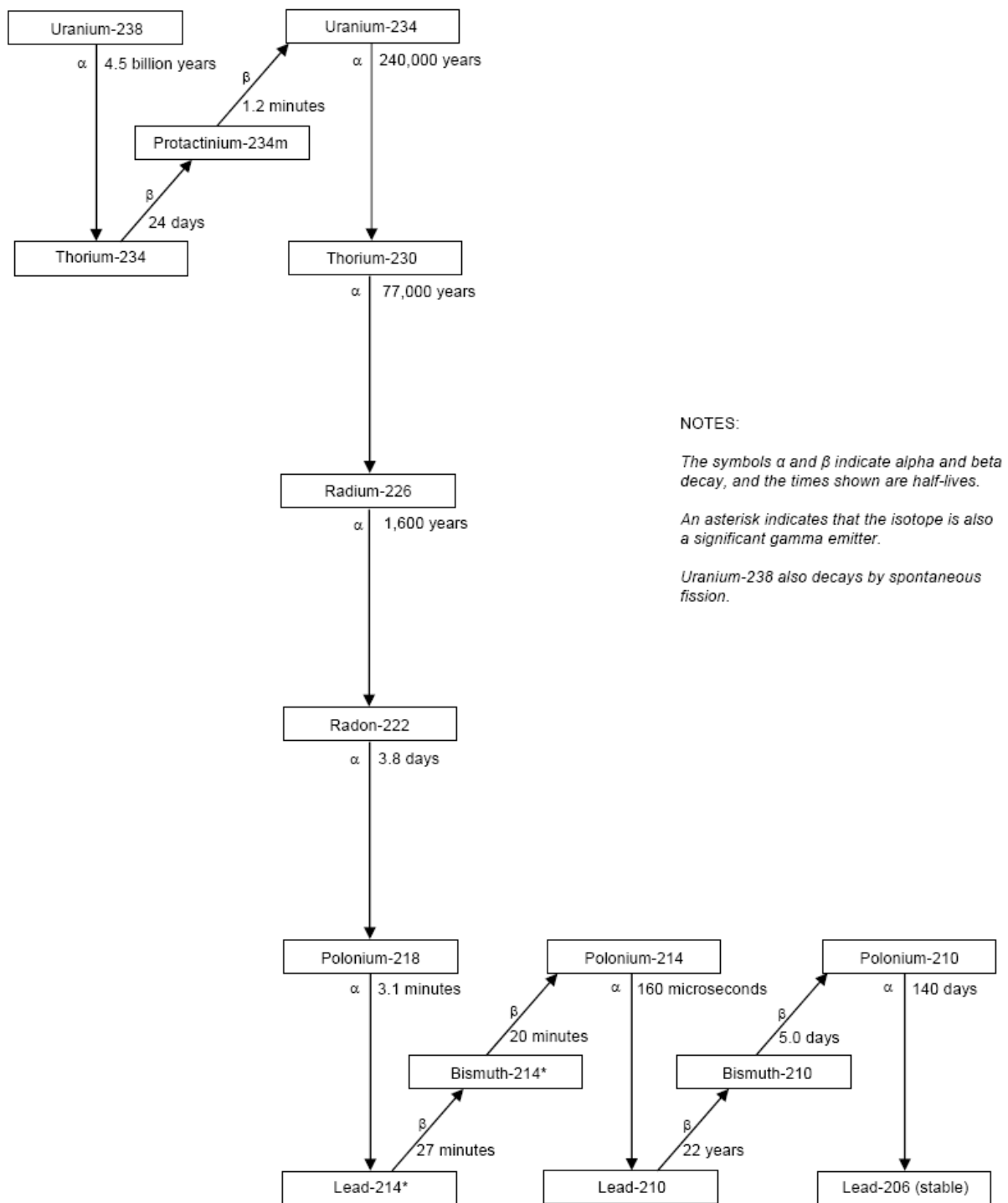
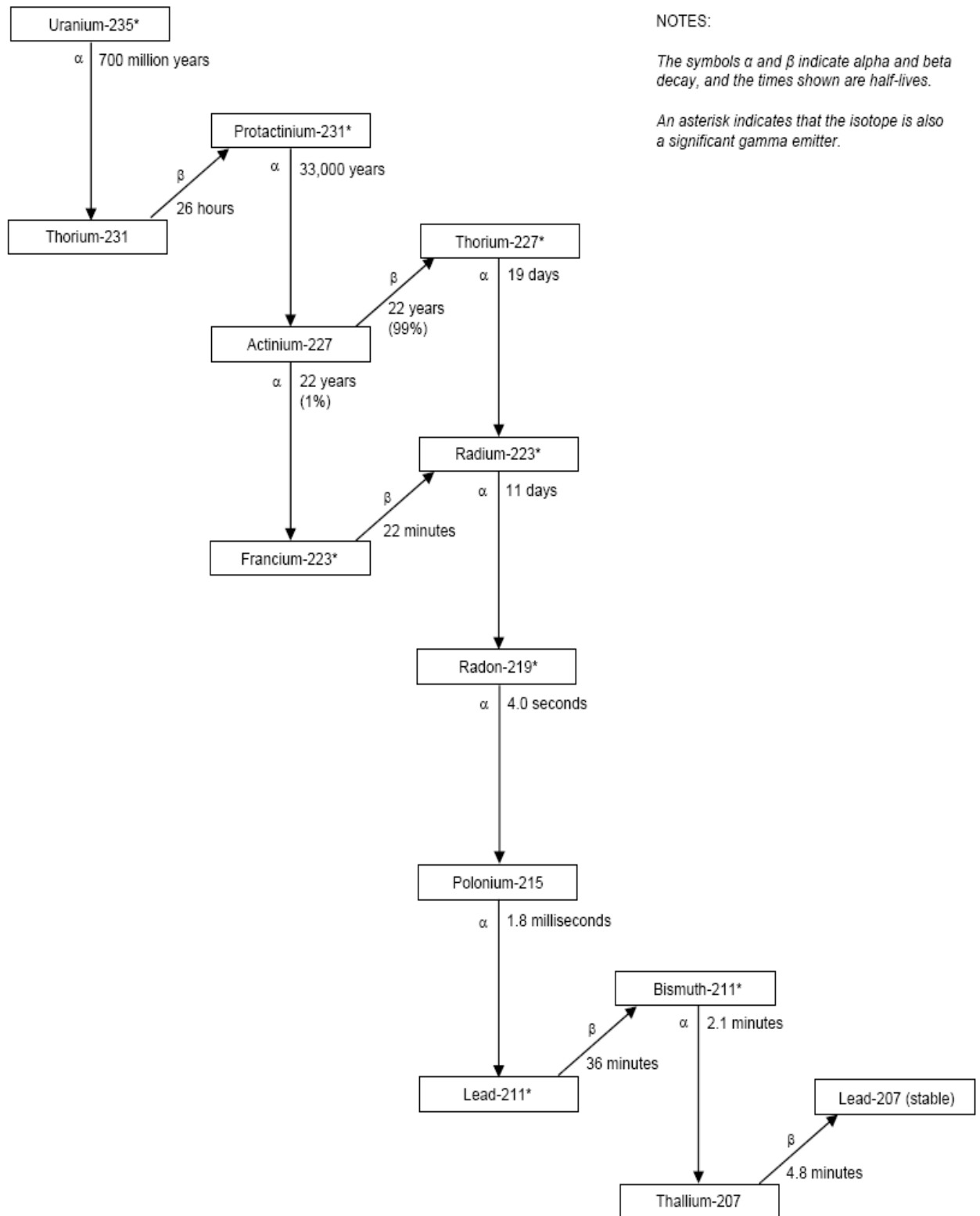


Figure 3.1: Natural Decay Series: Uranium-238 (Human Health Fact Sheet, 2005)



NOTES:

The symbols α and β indicate alpha and beta decay, and the times shown are half-lives.

An asterisk indicates that the isotope is also a significant gamma emitter.

Figure 3.2: Natural Decay Series: Uranium-235 (Human Health Fact Sheet, 2005)

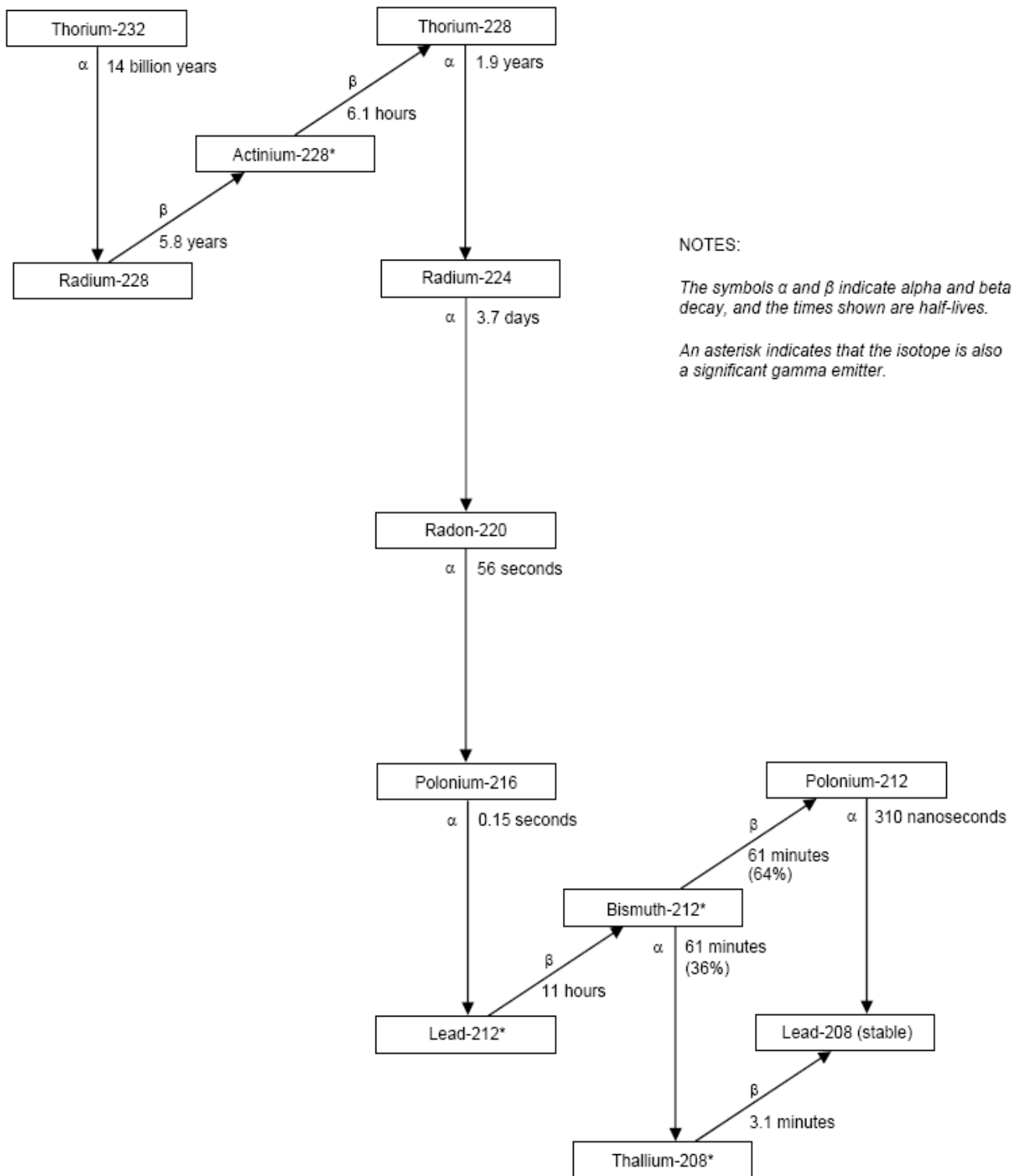
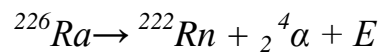


Figure 3.3: Natural Decay Series: Thorium–232 (Human Health Fact Sheet, 2005)

3.2 Radioactive Decay

Elements that are naturally radioactive include Uranium, Thorium, Carbon, and Potassium, as well as Radon and Radium. Uranium is the first element in a long series of decay that produces Radium and Radon. The genetic correlations of the radionuclides within the families are characterized by the terms “parent” and “daughter” (Lieser, 2001). Thus ^{238}U is the parent nuclide of all members of the Uranium family, ^{226}Ra is the parent nuclide of ^{222}Rn as shown in the following equation and ^{222}Rn is considered as daughter nuclide



The sequence of decay alternates either α decay is followed by β^- decay or β^- decay is followed by α decay (Lieser, 2001). While the final members of the decay series of Uranium and Thorium are stable nuclides such as lead-206 (^{206}Pb), lead-207 (^{207}Pb), and lead-208 (^{208}Pb).

The decay of each radioactive element occurs at a very specific rate. Rates of radionuclide decay are usually expressed in terms of half-life. This is the time t required for one-half of a certain number of nuclei to decay. The half-life of a radionuclide does not depend on pressure, temperature, state of matter or chemical bonding. Radionuclide decay may be defined in mathematical terms as the number (ΔN) of atoms disintegrating in a given time (Δt) is proportional to the number, N , of radioactive atoms present (Annunziata, 2003).

This relationship may be written as: $\Delta N / \Delta t = \lambda N^*$ or

$$dN / N = - \lambda dt^*$$

* Annunziata, 2003

Which can be integrated between the limits N_o and N and between t_o and t , where t_o is 0, N_o is the number of atoms originally present at time t_o , and N is the number of atoms remaining after time t . Where λ is a proportionality constant, commonly referred to as the decay constant (dimensions s^{-1}), and the negative signifies a decreasing number of radionuclide with time.

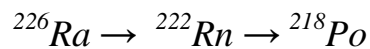
$$\ln N/N_o = -\lambda t^*$$

and the above equation could be written in exponential form as

$$N = N_o e^{-\lambda t^*}$$

During the series of transformations between the nuclides, the decay series can be written in the following form

nuclide 1 \rightarrow nuclide 2 \rightarrow nuclide 3



where $T_{1/2}(^{226}\text{Ra}) = 1600$ years and $T_{1/2}(^{222}\text{Rn}) = 3.8$ days.

where nuclide 1 is transformed by radioactive decay into nuclide 2, and nuclide 2 is transformed by radioactive decay into nuclide 3. At any instant, the net production rate of nuclide 2 as an intermediate nuclide is given by the decay rate of nuclide 1 decreased by the decay rate of nuclide 2:

$$dN_2 / dt = \lambda_1 N_1 - \lambda_2 N_2^{**}$$

** Lieser, 2001

Secular equilibrium can occur only in a radioactive decay if the half-life of the daughter radionuclide is much shorter than the half-life of the parent radionuclide, so

$$dN_2 / dt = 0 \quad \text{or}$$

$$\lambda_1 N_1 = \lambda_2 N_2$$

$$N_2 \approx \frac{\lambda_1}{\lambda_2} N_1$$

The concentrations of radioactive isotopes in a closed system will reach secular equilibrium or radioactivity equilibrium with the parent nuclide when the rate of formation equals the rate of decay (Webster et al., 1995). This secular equilibrium between parent and daughter implies an activity ratio of 1. So this implies that all the activities of the mother nuclide and all the nuclides emerging from it by nuclear transformation are the same as this is also valid for all the following radionuclides of the decay series. When the system is in an initial disequilibrium in the chain reaction that is $\lambda_1 N_1 \neq \lambda_2 N_2$, it is generally stated that the system will return to secular equilibrium after about six half lives of the daughter (Webster et al., 1995).

3.3 Types of Environmental Radioactivity

All living creatures from the beginning time have been and are still being exposed to radiation. Natural radiation and environmental radioactivity provide the major source of human exposure which comes from natural and artificial sources. Exposure to natural radiation is not uniform throughout the world and can vary substantially from place to place (Charles, 2001).

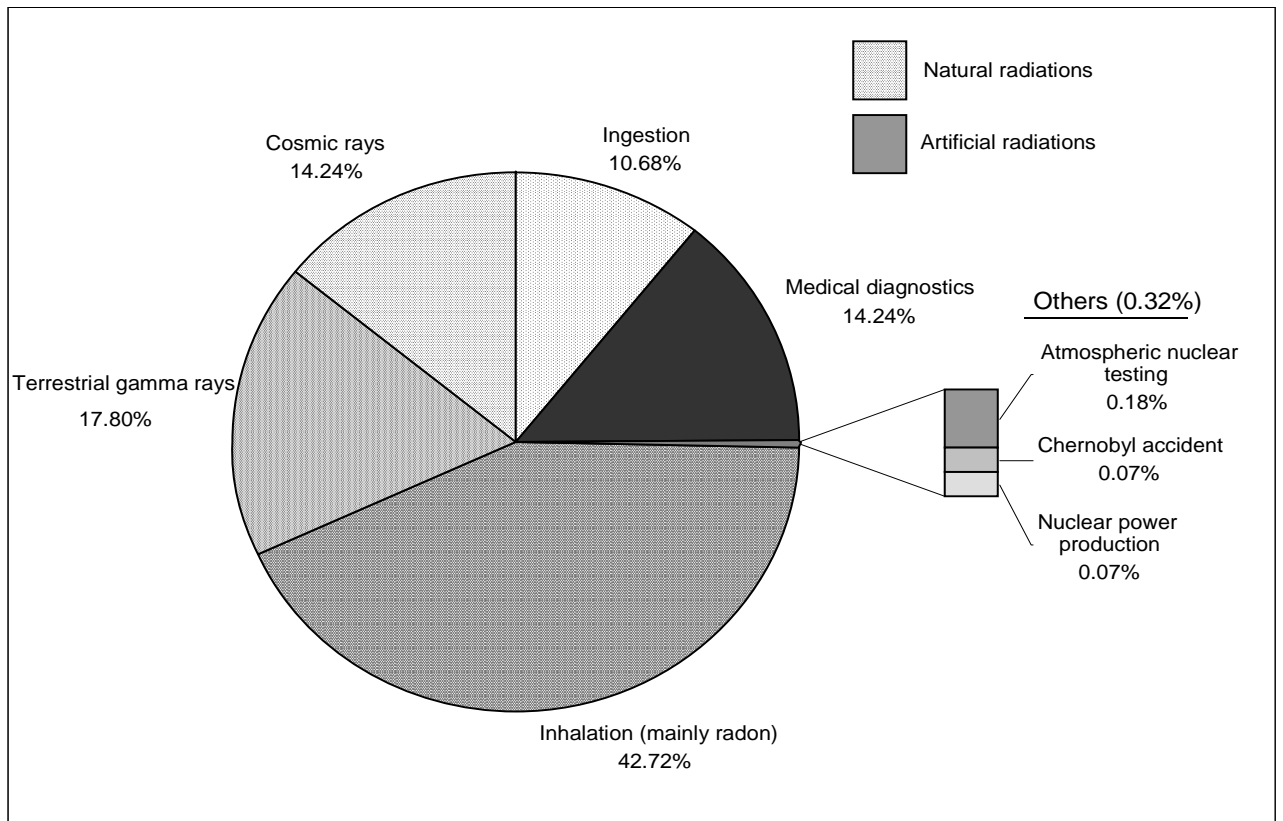


Figure 3.4: Pie chart showing the relative contributions from natural and man-made sources of radiation worldwide (Charles, 2001).

The difference between human-made sources of radiation and naturally occurring sources is the place from which the radiation originates. Social and industrial activities of the human beings has always changed this natural exposure and introduced new sources of radiation into the environment via the redistribution of natural activity (such as mining and minerals processing activities) or through the creation of man made radiation (such as medical X rays, nuclear power and weapons testing) (Guy, 1988). In Figure 3.4 shows that the natural sources of radiation account for about 85% of all public exposure (inhalation radon, ingestion, terrestrial and cosmic), while man-made sources account for the remaining 15% .

Radioactivity can be divided into four different types (Eisenbud and Gesell, 1997) and these can be placed into four categories:

- Cosmic radiation
- Cosmogenic –formed as a result of cosmic ray interactions
- Primordial –formed before the creation of the Earth
- Man made – which is produced by human activities

3.3.1 Sources of Natural Radiation Exposures

The two main sources of natural radiation exposures are:

- Sources of extraterrestrial origin of radiation (such as cosmic rays).
- Sources of terrestrial origin (such as radionuclides in the earth's crust, atmosphere, biosphere and hydrosphere).

3.3.1.1 Cosmogenic Radionuclides

Cosmogenic radionuclides are produced mainly by activation. When high energy cosmic nucleons interact with atmospheric gases (e.g. Nitrogen, Oxygen and Argon) in the stratosphere, troposphere, lithosphere and biosphere. The major sources of their production are the interactions involving the atmosphere.

Cosmogenic radionuclides appear to have relatively homogeneous distribution across the earth and have been detected in humans, topsoil, polar ice, surface rock, sediments, biosphere, sea floor and atmosphere. The four cosmogenic radionuclides contributing to the majority of the dose to humans are ^{14}C , ^3H , ^{22}Na and ^7Be (Natural Radiation, Human Sources).

3.3.1.2 Primordial nuclides

Primordial nuclides that originated in the early stages of the universe are even now present on the earth in a significant quantity due to their long half-lives. For example ^{238}U ($T_{1/2} = 9.51 \times 10^9$), ^{235}U ($T_{1/2} = 6.96 \times 10^8$), ^{232}Th ($T_{1/2} = 1.41 \times 10^{10}$), ^{40}K ($T_{1/2} = 1.28 \times 10^9$), ^{87}Rb ($T_{1/2} = 1.28 \times 10^9$). The three radioactive decay series (^{238}U , ^{232}Th and ^{235}U) have several common characteristics; the parent radionuclide of each has a long half-life, each series has a gaseous isotope of Radon and each series ends with a stable isotope of Lead.

Due to the ubiquitous presence of primordial radionuclides and their decay products in the environment (air, water, soil and foodstuffs) in the humans, they contribute between 80 – 90 % of the total natural background radiation dose to the human population.

3.3.2 Sources of Artificial Radioactivity – Anthropogenic Radionuclides.

Anthropogenic radionuclides are man-made radionuclides released into the environment through the testing of nuclear weapons and in the radioisotope manufacturing industry such as (^{137}Cs , ^{90}Sr and ^{131}I). A number of man's activities involve the use of radioactive materials. The most important of these is the use of radioactive materials for medical applications such as the diagnosis and treatment of cancer patients (Guy, 1988).

Some good manufactures contain small radioactive sources such as smoke detectors. Energy production such as nuclear energy production, extraction of oil and natural gas, and burning coal involves in the release of small amounts of radioactivity to the environment. There is also a low level of residual radioactivity in the environment from the nuclear bomb tests of the 1950s and 1960s. A severe nuclear accident, like Chernobyl, can add to this man-made radioactivity in the environment (Defra, 1999).

The variability of man-made sources of radiation and radioactivity is related directly to the population distribution and the level of technology found in different areas around the

world. Deposition in an area depends upon wind and precipitation conditions (NCRP, 1994).

3.4 Radium in groundwater

Radium occurs as a natural component of all groundwater in an extremely wide range of activities. This element rarely occurs alone, but as a rule it is generated by the decay of the natural Uranium and Thorium (Oliveira, et al., 1998).

Most radionuclides in groundwater result from interactions with rocks. The concentration of Radium in groundwater depends on the means by which it enters the water, the amount of Radium in the source, the mechanisms that remove Radium from the water and processes that move the Radium away from its source (Oliveira, et al., 1998).

The contents of Radium and its progeny radioactive elements in groundwater depend on the combination of three factors: (Vengosh, 2006)

- Geological factor including the concentrations of these elements in the aquifer rock.
- Chemical condition of the groundwater.
- Physical processes of decay along the water-rock interface.

3.4.1 Geological Factor

The first factor that determines occurrence of radioactivity in the groundwater is the geology of the aquifer. High abundances of parent elements of the decay chains are typically associated with high activity of one or several radionuclides in the associated groundwater. Sedimentary rocks, such as shale and phosphate rocks are predominantly enriched in Uranium and thus the decay daughter of Uranium decay chain, ^{226}Ra , characterizes the associated groundwater (Vengosh, 2006). Similarly, silica-rich igneous

rocks, such as granite, are enriched in both Uranium and Thorium, and so associated groundwater contains their decay products, ^{226}Ra and ^{228}Ra (Vengosh, 2006).

Thus measuring the Radium isotopes will allow determining the magnitude of radioactivity including short and long term isotopes, which enable us to show their origin, since the combination of isotopic ratios reflects the Radium sources. The Radium isotopes ratio can be used to draw their origin especially in ground water. The ratio of the Radium isotopes $^{226}\text{Ra} / ^{228}\text{Ra}$ depends upon their host rock origin. As ^{226}Ra is the descendent of ^{238}U and ^{228}Ra is of the ^{232}Th , so the ratio $^{226}\text{Ra} / ^{228}\text{Ra}$ reflects the ratio of the rock surface as well as the rock itself (Porcelli and Swarzenski, 2003). For example in most cases ground water in carbonate aquifers has high ratio $^{226}\text{Ra} / ^{228}\text{Ra} > 1$ while in ground water in sandstone aquifers have low ratio $^{226}\text{Ra} / ^{228}\text{Ra} < 1$ (Sturchio, et al., 2001).

3.4.2 Chemical Factor

The second factor that controls mobilization of radionuclides from the aquifer rocks is the chemical condition of the groundwater, which can result in significant leaching of these elements into groundwater (Vengosh, 2006). Groundwater also plays a role in the migration and redistribution of the elements in the Earth's crust. Some characteristics of water that mainly determine its capacity to dissolve, carry or deposit elements are its pH, temperature, redox potential, concentrations and properties of dissolved solids, and flow rate (Asikainen, 1981).

The geochemical properties of each radionuclide determine its availability in water. Radium can be kept out of groundwater by sorption onto clay minerals, precipitation with secondary minerals and radioactive decay. As the abundance of Radium naturally is low in surface water 10^{-12}g/L , so it is rarely that Radium salts reach solubility product concentration in natural surface water (Oliveira, et al., 1998). Therefore, the important

chemical reactions for Radium are those of adsorption to active surfaces of all kinds and co-precipitation with Ca and Ba salts in particular. In few cases co-precipitation with Mg, Fe and Mn can occur (Oliveira et al., 1998).

Many studies have shown that an exchange reaction with clay minerals is the predominant process that controls the Radium activity in low-saline groundwater. The ratio of Radium adsorbed on sediments to dissolved Radium in solution decreases with the increase of the ionic strength of the solution (Porcelli and Swarzenski, 2003). So this means that in fresh water conditions, Radium concentration or activity will be decreased as the Radium is retained to the aquifer solids, while in high saline water Radium is rapidly desorbed and the Radium concentration increased (Zukin, et al., 1987). The increasing Radium concentrations in saline groundwater have been interpreted as a result of competition between Radium and cations for adsorption sites on solids, resulting in Radium solubility enhancement (Moore and Shaw, 1998).

Studies showed that Radium readily dissolves in groundwater where acid conditions (low pH levels) are found (Almeida, et al., 2004). Other studies have established that groundwater with no oxygen is typically enriched in Radium. The high Radium activity in oxygen-free water seemingly comes from the mobilization of manganese. With oxygen present, Radium strongly bonds to manganese oxide and yet in oxygen-free conditions, manganese oxide is no longer stable, and both Radium and manganese are released into the associated groundwater. Therefore reducing conditions is another factor that control Radium activity in ground water. The anoxic conditions where the Mn and other oxides are reduced as they are important factors in precipitating Radium, thus leading to the release of Radium in the aqueous solution (Dickson, 1985). This means that Radium

concentration is high in low Eh conditions due to absence of MnO₂ that can strongly adsorb Ra⁺² (Zukin, et al. 1987).

3.4.3 Physical Factor

The third factor affecting movement of radionuclides into groundwater is physical. Due to high kinetic energies that are associated with radioactive decay, daughter isotopes typically move from the parent isotopes within the rock into the water, in a process known as recoil. Alpha recoil is a process by which a radioactive daughter is mobilized from its initial position by the energy of the alpha decay. Since beta recoil energy is less than 0.1 KeV so it is negligible comparing to alpha recoil energy > 60 KeV where (1eV = 1.6022 x 10⁻⁹ J). A Radon molecule is formed when a Radium molecule releases an alpha particle and turns itself into a Radon molecule. The Radon molecule is recoiled away from the alpha particle that is formed (Air & Water Quality Inc., 2000). The recoil causes the Radon to be driven into the water as shown in Figure 3.5. Radon is injected into the water by the decay of Radium.

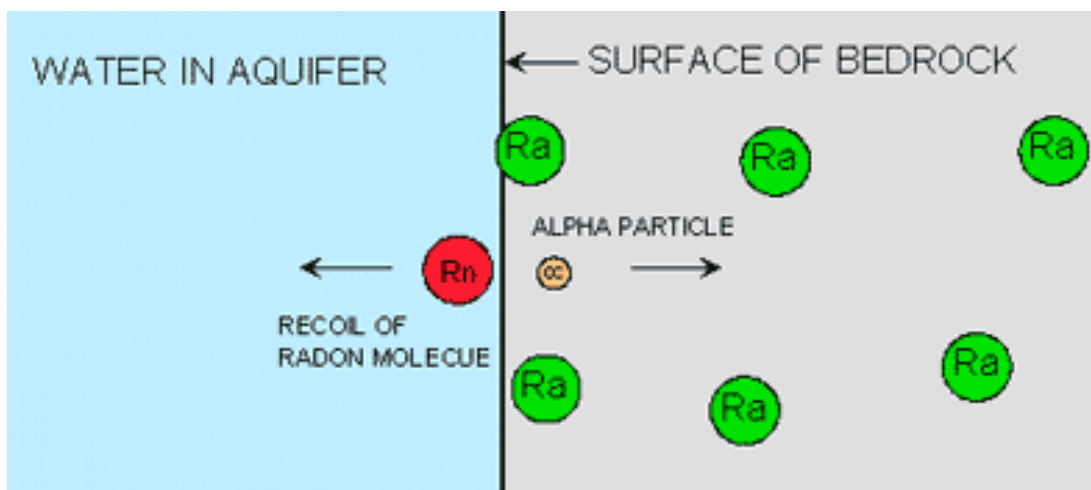


Figure 3.5: The recoil process of Radon in groundwater (Air & Water Quality Inc., 2000)

Radon and other isotopes in the Uranium–Thorium series are introduced into nanopore water as a result of recoil from the walls of the nanopores in solids. Radon, an inert gas, is able to diffuse out into intergranular water while the reactive isotopes are adsorbed within the nanopores as illustrated in Figure 3.6.a and 3.6.b (Rama and Moore, 1984).

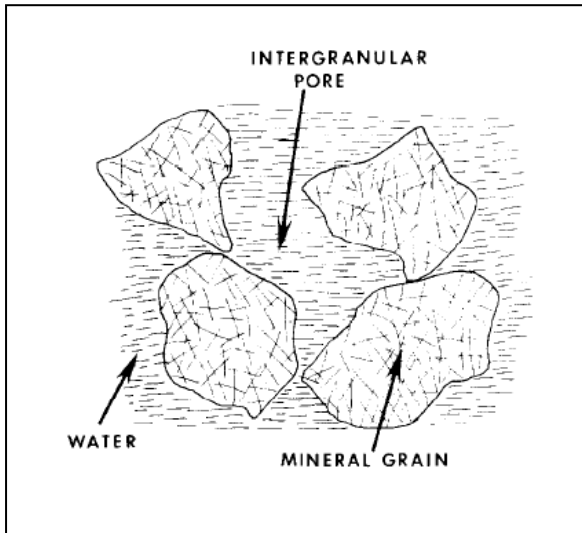


Figure 3.6.a: Schematic diagram of nanoporosity in solids found in aquifers (Rama and Moore, 1984).

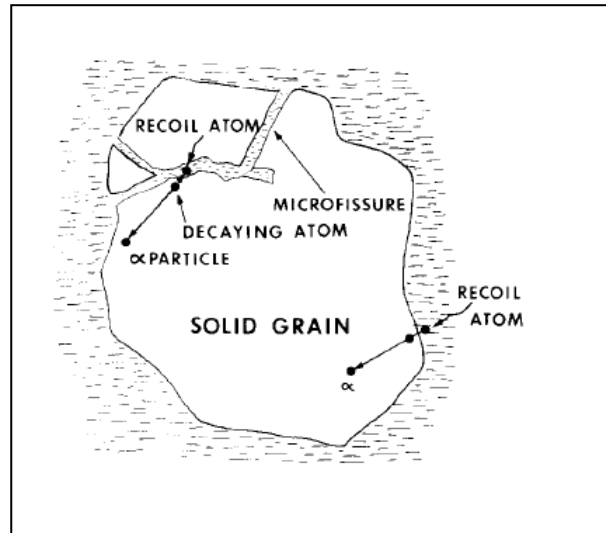


Figure 3.6.b: Schematic diagram of Radon and other U-Th series isotopes enter the nanopores by recoil (Rama and Moore, 1984).

The relationships between the radioactive decay rates of the radionuclides and the flow rate of the groundwater will determine the amount of radioactivity that is added to the water by this mechanism. Stagnant and old groundwater, for example, is generally enriched in both short- and long-lived isotopes, given the long contact time between water and the aquifer rocks (Vengosh, 2006). And because of increased contact between rocks and water in the cracks, extremely high levels of Radon in groundwater typically occur in association with fractured granite rocks. A very slow flow rate of groundwater in an aquifer is the ideal setting for maximizing the recoil effect. Thus, in very low-gradient aquifer systems, the recoil process may have an important effect on groundwater radioactivity. Alpha recoil is a

physical process and is unlikely to be affected substantially by a change in water chemistry (Martin and Akber, 1999).

3.5 Units of measurement for Radium elements in water

Radioactive emissions are measured by an activity unit called a Curie (Ci), the common representation of water activity is the picocurie (pCi), equal to 10^{-12} Ci, where 1dpm (disintegrations per minute) per liter of water is equal to 2.2 pCi. Activity in water is also expressed in International System of Units (SI unit) which is the Becquerel (Bq), where 1 Bq equals 1disintegration per second. For drinking water the guidance levels are often given as the activity of the radionuclide per liter (Bq/L), called the activity concentration.

$$1 \text{ dpm/L} = 2.2 \text{ pCi/L}$$

$$\text{Bq/L} = \text{dpm/L} \div 60$$

$$1 \text{ pCi/L} = 0.037 \text{ Bq/L}$$

The absorbed dose refers to how much energy is deposited in material by the radiation. The measurement of the quantity of radiation received or dose absorbed by a person or a mass of matter is expressed in grays. $1 \text{ Gy} = 1 \text{ joule per kilogram (J/kg)}$.

3.6 Maximum Permissible Concentrations of Radium and Radon in drinking water.

Environmental Protection Agency (EPA) regulations set the drinking water standard at an average annual concentration of gross alpha particle radioactivity in drinking water to 15 pCi/L and the average annual combined concentration of ^{226}Ra and ^{228}Ra to 5 pCi/L (0.185 Bq/L). Both ^{223}Ra and ^{224}Ra may contribute to the gross alpha activity of water measured soon after drawing from the tap, however their contributions to the long term dose deposited in the skeleton are negligible because they have short half lives (Alabdula'aly, 1999). While the recommended safe limit of Radon in drinking water is between 4 – 40 Bq/L (Singh et al., 2008).

For ^{226}Ra and ^{228}Ra , the United States EPA estimates that the additional lifetime risk for cancer associated with drinking water containing 5pCi/L is about 1 in 10,000. According to the EPA model, as the level of Radium increases, so does the risk. So this means that the risk doubles to 2 in 10,000 at 10 pCi/L and triples to 3 in 10,000 at 15 pCi/L. This means that if 10,000 people were to consume two liters of this water per day for 50 years, one additional fatal cancer would be estimated among the 10,000 exposed individuals.

3.7 Radioactive elements impact on human health.

Radium like other elements of the earth's crust naturally enters the body through drinking water and food. Radium radioactivity in drinking water is particularly important as Radium has a similar metabolic behavior as calcium in the body, and because of this similar metabolism, ingestion of trace quantities of Radium over time will result in an accumulation of Radium in the skeleton. Radium that has accumulated in bone tissue decays into a series of short-lived daughter products, resulting in the emission of a number of alpha and beta particles over a short time span. As Radium and its daughters decay, the energy produced by the radiation can strip electrons from the atoms with which it collides. These stripped electrons have a great capacity to break chemical bonds as they travel through living tissue, causing the release of additional electrons. The atoms in living tissue that lose electrons become ions at a high energy state capable of producing chemical reactions that would not have been otherwise possible, resulting in damage to bones and other living tissue as well as genetic material inside the tissue. Ultimately, the damage from continuous exposure to Radium can potentially cause bone and sinus cancer (Jacomino et al., 1996).

Chapter Four

Literature Review

- Rama and Moore (1984) in Mechanism of transport of U-Th series radioisotopes from solids into groundwater where they conducted a series of experiments to understand the mechanism responsible for release of large quantities of ^{222}Rn from solids into groundwater. Radon and other isotopes in the U-Th series are introduced into nanopore water as a result of recoil from the walls of the nanopores in solids. Radon, an inert gas, is able to diffuse out into intergranular water while the reactive isotopes are adsorbed within the nanopores. This reveals that a major part of Radon moving into the intergranular water comes from within the grains (solids) not from the outer surface.
- Dickson (1985) in his paper Radium isotopes in Saline Seepages, South-Western Yilgarn, Western Australia aimed to establish a relationship between the source rocks and Radium isotopic ratios and to examine the factors controlling the mobilization of Radium. In his study, the concentrations of these Radium isotopes in ground and surface waters were compared with the parent Uranium and Thorium concentrations of possible source rocks. The probable source rocks of the Radium, gave Th/U activity ratios of around 1.5 leads to the higher $^{228}\text{Ra}/^{226}\text{Ra}$ ratios of the waters. Solutions containing high concentrations of cations can exchange Radium from a solid phase into solution. Sulphate anions can decrease this exchange as the decrease may represent prevention of exchange by formation of RaSO_4 complexes which are unable to diffuse from the rock matrix. Where as a decrease in pH can significantly increase the exchange. The laboratory studies demonstrate that

Radium transfers into solution by cation exchange processes are dependent on the composition of the groundwater.

- Zukin et al. (1987) in Uranium-Thorium series radionuclides in brines and reservoir rocks from two deep geothermal boreholes in the Salton Sea in southeastern California explained that the Uranium and Thorium decay series include many isotopes with different chemical properties and mean lives. It was suggested that high Radium concentrations in saline waters resulted from the displacement of Radium on clay mineral surfaces by other cations such as Na, Ca, Ba, and Mn. The results showed that Radium concentrations may also be high in low Eh conditions due to the absence of MnO₂ that can strongly adsorb Ra⁺² and due to low SO₄⁻² concentrations that prevent formation of RaSO₄. High temperature may also play a role because adsorption coefficient (K_d) should decrease with increasing temperature, thus Radium, Radon and Lead are soluble and relatively mobile in the geothermal aquifer system.
- Dickson and Herczeg (1991) in Naturally-occurring radionuclides in acid-saline groundwater's around Lake Tyrrell in Australia had showed that the main objectives of their studies were to determine the source of ²²⁶Ra which produces the radioactive area, and to determine the effects of high salinities and low pH on the mobility of a variety of radionuclides within the ²³⁸U and ²³²Th series. They concluded as a result of their study that many daughter radionuclides of the U and Th decay series are mobilized by the acid-saline groundwaters found near the lake. In contrast, the parent elements are relatively immobile.
- Copenhaver et al. (1993) in Retardation of ²³⁸U and ²³²Th decay chain radionuclides in Long Island and Connecticut aquifers declared that the knowledge of the ability

of an aquifer to retard the groundwater transport of toxic or radioactive ions can be deduced from the analysis of groundwater for the radionuclides of the ^{238}U - and ^{232}Th -decay chains. The natural ^{238}U and ^{232}Th decay series contain a number of radionuclides with different modes of decay, half-lives, and chemical properties. These properties make the ^{238}U and ^{232}Th series nuclides suitable for determining sorption characteristics of aquifers. Properties such as the nature of the aquifer solids and the pH, salinity, oxygen content, and ligand chemistry of the water all act to determine the retardation of an ion.

- Martin and Akber (1999) in Radium isotopes as indicators of adsorption-desorption interactions and barite formation in groundwater had studied the isotopes of Ra, Th, and Ac measurements in bore water well near the Ranger U mine tailings dam. The concentrations of ^{223}Ra , ^{224}Ra and ^{228}Ra as well as the nucleidic ratios $^{228}\text{Ra}/^{226}\text{Ra}$, $^{223}\text{Ra}/^{226}\text{Ra}$ and $^{224}\text{Ra}/^{228}\text{Ra}$ generally increased. It was concluded that increases in Ra isotope concentrations arise from the competition for cation adsorption sites in the vicinity of the bore rather than direct transport of Ra from the tailings. Formation of a barite solid phase (BaSO_4) occurs in the groundwater and causes the removal of some Radium from the solution, with rapid replenishment of the shorter-lived isotopes from their parents.
- Kim et al. (2001) in his paper Measurement of ^{224}Ra and ^{226}Ra Activities in Natural Waters using a Radon-in-Air Monitor such as RAD-7 where they report a new technique for measuring low level radium isotopes (^{224}Ra and ^{226}Ra) in natural waters. The radium present in natural waters is first preconcentrated onto MnO_2 -coated acrylic fiber (Mn fiber) in a column mode. The radon produced from the adsorbed radium is then circulated through a closed air-loop connected to a

commercial radon-in-air monitor. The monitor counts alpha decays of Radon daughters (polonium isotopes) which are electrostatically collected onto a silicon semiconductor detector. ^{224}Ra is measured immediately after sampling via ^{220}Rn (^{216}Po), and ^{226}Ra is measured via ^{222}Rn (^{218}Po) after a few days of ingrowth of ^{222}Rn . This technique is rapid, simple, and accurate for measurements of low-level ^{224}Ra and ^{226}Ra activities without requiring any wet chemistry. Rapid measurements of short-lived ^{222}Rn and ^{224}Ra , along with long-lived ^{226}Ra , may thus be made in natural waters using a single portable system for environmental monitoring of radioactivity as well as tracing of various geochemical and geophysical processes.

- Sturchio et al. (2001) in Radium geochemistry of ground waters in Paleozoic carbonate aquifers, midcontinent, USA, showed the processes controlling the distribution and behavior of the longer-lived Radium isotopes in continuous Paleozoic carbonate aquifers. Activities of ^{228}Ra and ^{226}Ra were analyzed in fresh and saline groundwater, brines, and rocks. The ^{226}Ra activity correlates with salinity and other alkaline earth element (Ca, Sr, and Ba) concentrations. The relatively low mean fluid ratio ($^{228}\text{Ra} : ^{226}\text{Ra}$) reflects the low Th:U ratio of the predominant carbonate aquifer rock. Radium occurs mostly as Ra^{+2} species in the fluids.
- Choubey et al. (2003) in their paper Radon in groundwater of eastern Doon valley, outer Himalaya found that the Radon content in water may serve as a useful tracer for several geohydrological processes. The presence of Radium in host rocks as well as the soil porosity and permeability control the Radium concentration in groundwater. As a result there exists a significant positive correlation between

Radon concentration and depths of the wells, suggesting that Radon concentration increases with drilling depth in certain areas. However, there is no correlation between Radon concentration and temperature, pH and conductivity.

- Moon et al. (2003) in Preconcentration of Radium isotopes from natural waters using MnO₂ Resin had showed that the sorption characteristics of Radium and Barium are highly dependant on pH with the most useful range from pH 4 to 8. The surface layer of Mn oxides is positively charged due to the presence of proton excess under acidic conditions (below pH 4) which prevents diffusion of positively charged alkaline earth species such as Ba⁺², Ra⁺² into the surface layers. It is thought that at higher pH adsorption will be inhibited because of carbonate complexation. While the sorption kinetics between Ba (Ra) and MnO₂ Resin are rapid for low-salinity waters such as deionized and groundwater, sorption rates decrease as the salt concentrations in solution increase. This indicates that the free sorption sites on the MnO₂ Resin are being competed for by alkaline earth elements common in natural waters such as Mg²⁺, Ca⁺², Sr⁺².
- Almeida et al (2004) in Groundwater radon, Radium and Uranium concentrations in Regiao dos Logos, Rio de Janeiro State in Brazil , analyzed groundwater for ²²⁶Ra , ²²⁸Ra ²²²Rn, ²³⁸U and major ion concentrations, and physico- chemical parameters. They found that the most important water parameter is low pH value linked to high Radium concentration, probably related to limited adsorption of Radium on soil ferric oxides and hydroxides. The low pH value has a direct impact on adsorption behavior of Radium. Ferric oxides and hydroxides abundant in tropical soils have a positive charge at low pH range and Radium present in cationic form as Ra⁺² is not adsorbed and remains in groundwater

- Spizzico (2005) in his paper Radium and Radon content in the carbonate-rock aquifer of the southern Italian region of Apulia, showed in his studies that high concentrations of ^{222}Rn have been found throughout the waters of the coastal carbonate-rock aquifer in the region Apulia in southern Italy. His studies had determined that such concentrations are due to the radioisotopic features of terra rossa, generated as a residual by-product of carbonate dissolution and is found to be widespread throughout the aquifer's fissures and karst cavities. In fact there are important differences in ^{222}Rn concentrations found in waters that come in contact with this type of rocks. The partial dissolution of some carbonate rock samples confirmed that the ^{226}Ra released by the dissolved rock primarily accumulates in the residual soil deposits, especially in those containing finer granules. It has been found that the ^{222}Rn concentrations in the water depend on the specific terra rossa ^{226}Ra activity rather than on the quantity of terra rossa.
- Skeppström and Olofsson (2006) in their paper A prediction method for Radon in groundwater using GIS and multivariate statistics found that high Radon concentrations in groundwater are not always associated with high Uranium content in the bedrock, since groundwater with a high Radon content has been found in regions with low to moderate Uranium concentrations in the bedrock. Their results showed that Radon concentration was clearly correlated to bedrock type, well altitude and distance from fracture zones. The study showed that the occurrence and spread of Radon in groundwater are guided by multiple factors, which can be used in a Radon prediction method on a general scale. However, it does not provide any direct information on the geochemical and flow processes involved.

Chapter Five

Methodology

5.1 Sampling sites

The wells that are included in this study are located in the southern part of the West Bank, Bethlehem and Hebron district and they are found in the Eastern Groundwater Basin. A total of fourteen wells were sampled with time interval starting from November 2007 till August 2008. Most of them are from Bethlehem area, three wells are from Hebron area. All wells location is illustrated in Table 5.1 and Figure 5.1

Table 5.1: Sampling sites in Bethlehem and Hebron districts.

No	Name	Locality	Aquifer	X - Coordinate	Y - Coordinate	Well depth (meters)
1	Herodion (1)	Bethlehem	Upper	170894	118278	350
2	Al Fawar 1	Hebron	Upper	156200	098110	100.5
3	Hundaza	Bethlehem	Upper	169378	121401	330
4	Asamoua	Hebron	Upper	156212	98199	191
5	Herodion (3)	Bethlehem	Lower	170743	117296	800
6	Herodion (2)	Bethlehem	Lower	170930	119787	770
7	Herodion (4)	Bethlehem	Lower	169450	114080	691
8	PWA I	Bethlehem	Lower	167375	112395	600
9	PWA 11	Bethlehem	Lower	164194	116411	851
10	Izzariya (1)	Bethlehem	Lower	174348	124082	996
11	Izzariya (2)	Bethlehem	Lower	173860	119880	793
12	Izzariya (3)	Bethlehem	Lower	175769	128525	835
13	JWC 4	Bethlehem	Lower	170877	121888	787.5
14	Al Rehea	Hebron	Lower	157250	96086	495

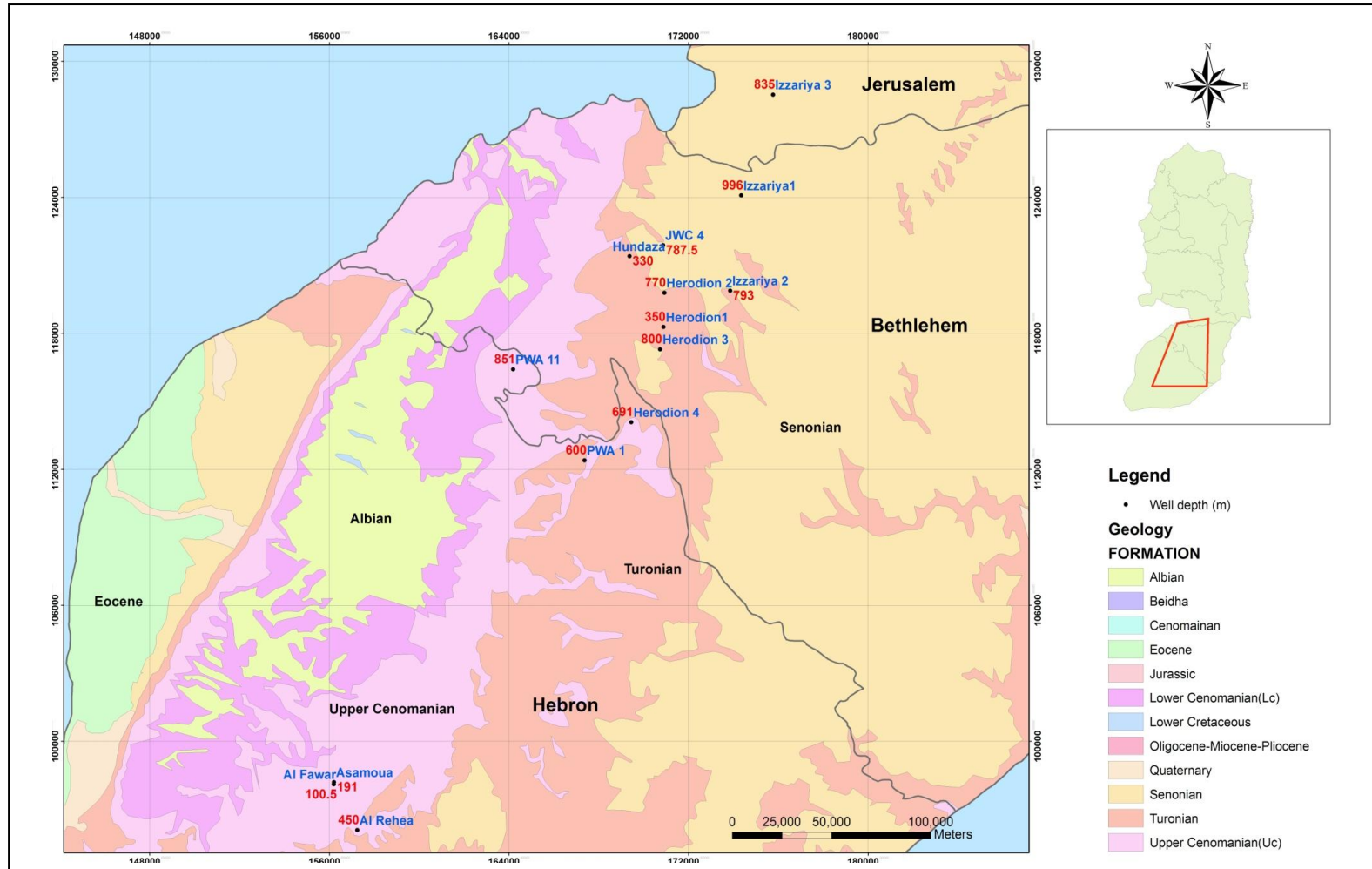


Figure 5.1: Location of the wells in Bethlehem-Hebron districts in the West Bank.

5.2 Sampling procedure

Radium and Radon sampling procedure had started from November 2007 till August 2008 in Bethlehem–Hebron districts. Our sampling procedures were divided into three categories depending on the type of analysis that our research demand.

5.2.1 Chemical sampling procedure

For the chemical sampling:

- Recording sufficient information on each bottle to provide positive sample identification such as the exact location of the sample, date, time and the name of the sample collector.
- Sampling procedure for general chemistry major ions (Ca^{2+} , Mg^{2+} , Na^+ , K^+ , NH_4^+ , Cl^- , SO_4^{2-} , HCO_3^- , NO_3^- , PO_4^{3-}) are collected in a one liter tightly closed plastic bottle already rinsed with the sampling water to avoid contamination.

5.2.2 Radium isotopes sampling procedure

For the Radium isotopes sampling the following instruction are taken into consideration:

- The Radium samplings are collected in a container (40- 50 L) with full information including date (days, hours, and minutes), site name, and exact volume of the sample.
- If the sample of water contains clay, seaweed and sand particles, the filtration process will be necessary through cotton wool to avoid altering the adsorption process.
- Water is pumped through a plastic column (30 cm in length) placed vertically, filled with 10 grams of MnO_2 coated acrylic fiber with a piece of cotton wool that is placed on the top of the fiber in order to prevent the loss of MnO_2 -fibers during the filtration.

- The pumping rate is less than 2L/ minute, in order to ensure 100% adsorption of dissolved Radium in the water sample to the MnO₂ fibers. When the whole water sample passes through the column, the MnO₂ fibers are squeezed strongly and place it in a plastic bag. If some of the cotton wool particles contain MnO₂ particles, it was placed in the plastic bag. Full information was written on the bag; name and code of the sample, sampling time, filtering time and volume of water sample. The following Figure 5.2 illustrates the filtration procedure.

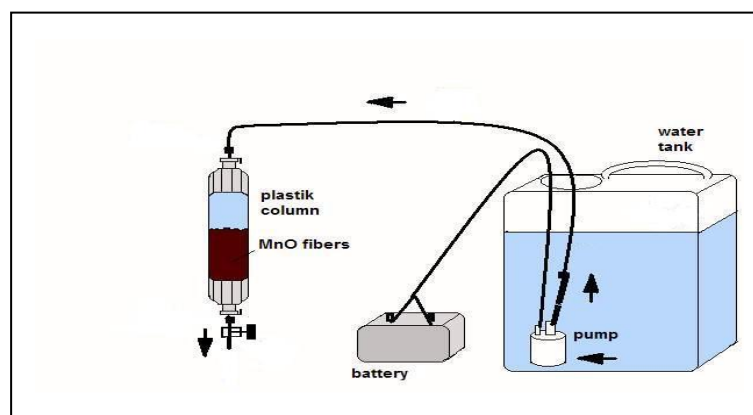


Figure 5.2: Technical circuit of the sample filtration used for Radium preconcentration.

5.2.3 Radon sampling procedure

Radon sampling procedure needs special care and practice. The sampling technique is the major source of error in measuring the Radon content of water. To avoid contact the sample with air, we had attached a rubber tube to the faucet after running the water several minutes, filling the bucket with water then we insert the vial under the water, fill it and close it tightly while it is still under the water. Be sure that no bubbles are found in the vial.

5.3 Measurements

5.3.1 Chemical analysis of water

The temperature, pH and EC were measured by using Multi 340 I pH-meter immediately at the sampling site. Cations (Ca^{+2} , Mg^{+2} , Na^+ , K^+) were measured by Atomic Absorption, while NH_4^+ and the main anions SO_4^- , PO_4^- , NO_3^- were measured by Hach spectrophotometer. Chloride Cl^- was measured by titration. Analysis of the water samples were conducted at the Water and Environmental Laboratory at Al- Quds University.

5.3.2 Radium isotopes analysis

The Durrige Radon- in -air monitor (RAD7) was used for the ^{226}Ra measurement as shown in Figure 5.3. This technique is rapid, simple and accurate for measurements of ^{226}Ra activities without requiring any wet chemistry. RAD7 uses a solid state alpha detector which is a semiconductor material usually silicon that converts alpha radiation directly to an electrical signal. The most advantage of solid state devices is its ability to electronically determine the energy of each alpha particle, thus make it possible to tell exactly which isotope (polonium isotopes) produced the radiation. Because of the high quality alpha detector the RAD7 background is vanishingly small.

^{226}Ra is measured via ^{222}Rn (^{218}Po) after three weeks of incubation and ingrowth of ^{222}Rn . After first preconcentrated the Radium onto MnO_2 - coated acrylic fiber in a column mode where the Radon produced from the adsorbed Radium is then circulated through a closed air-loop connected to a monitor. The monitor counts alpha decays of Radon daughters which are electrostatically collected onto a silicon semiconductor detector. Count data are collected in energy- specific windows, which eliminate interference and maintain very low backgrounds (Kim et al., 2001).

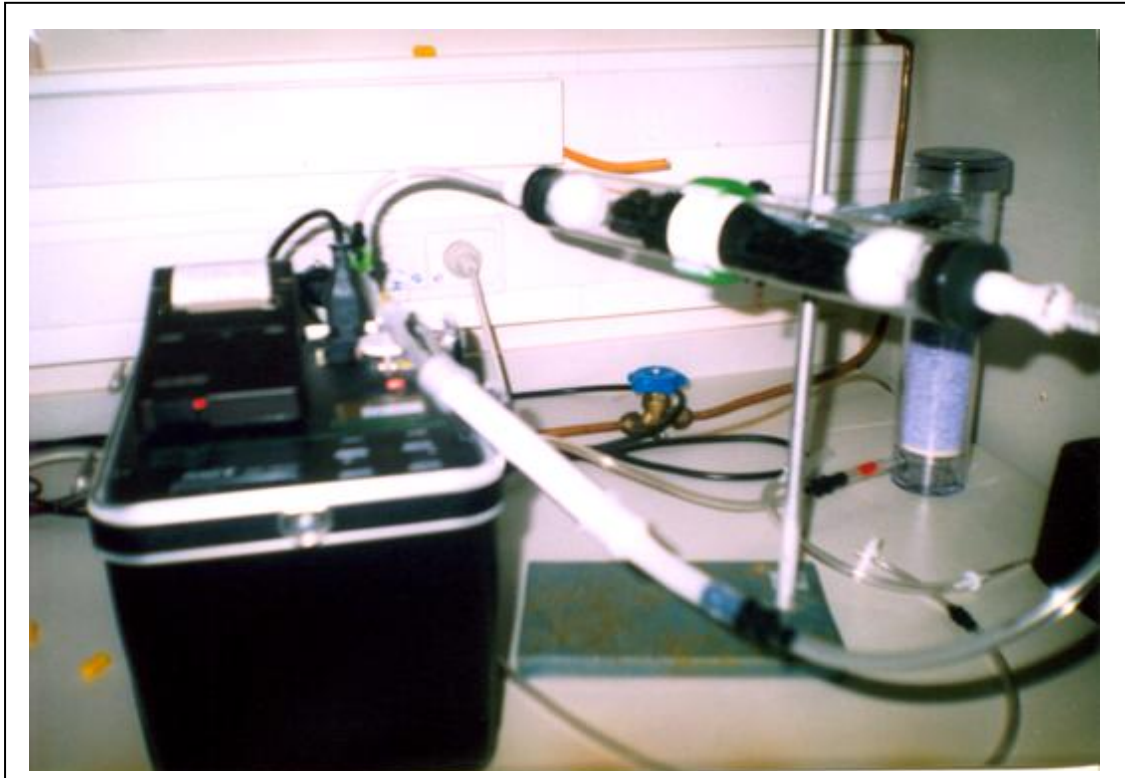


Figure 5.3: Close loop during ^{226}Ra measurements at Al Quds University.

5.3.3 Radon analysis

The measurement of radon was done by RAD7-H₂O which is an accessory to the RAD7 that enables to measure Radon in water with high accuracy over a range of concentrations from less than 50 pCi/L (1.85 Bq/L) to greater than 10⁵ pCi/L (3700Bq/L). The lower limit of detection is less than 10 pCi/L (0.37 Bq/L) (Durrige Company Inc., 2001). The setup consists of three components, the RAD7 on the right, the vial 250 ml of sampling water that we used in our study center in the front and the tube of desiccant on the top left. Figure 5.4 illustrates the RAD7-H₂O (Durrige Company Inc., 2001).

Before making any measurements, RAD 7 must be free of radon and dry by purging the unit with fresh air at least for ten minutes until the percentage of humidity reach 6%. Then stop purging, put on RAD-7 and choose protocol Wat-250 that we had used in our study.

We had entered the right protocol as this controls the pumping and counting cycle and the calculation according to the size of sample vial. When everything was ready the test started and the pump run for five minutes aerating the sample and delivering the radon to the RAD-7. The system had waited a further five minutes. Then it was started counting and repeating for another two times. At the end of the run (30 minutes after the start), the RAD-7 printed out the summary, showing the average radon reading from the four cycles counted, a bar chart of the four readings and a cumulative spectrum. The final step was correcting the measured value for decay of the radon in the water during the time taking the sample and analyzing it.



Figure 5.4: Radon measurement using RAD7- H₂O (Durrige Company Inc., 2001).

5.4 Calculations

The measurements process for ^{226}Ra and ^{222}Rn activities was conducted several times for obtaining better accuracy. Average of the cycles is taken in order to obtain one single value which is the mean in counts per minute (cpm) for ^{226}Ra and pCi/L for ^{222}Rn . The value taken from the Rad-7 must be corrected in order to take into consideration the amount that has been decayed in the period elapsing the date of sampling and the date of measurement. The percentage of the radionuclide remaining after a certain period of time is given by the following equation

$$K_i = e^{-\lambda_i t} = e^{-0.18 t}$$

K_i : Decay rate of radionuclide i

λ_i : Decay constant for radionuclide i and it is equal to $\ln 2/T_{1/2}$, where the $T_{1/2}$ is the half time of the radionuclide i ($T_{1/2}$ for ^{222}Rn is 3.82 days).

t : incubation time (t is the interval time between the time sampling and the time of measurement).

The measured value is simply divided by K_i to give the corrected cpm. The system efficiency must be incorporated into this value; this is obtained by using calibration samples with known activities and includes unit conversion factors to obtain a value in disintegrations per minute (dpm) and eliminates any background values that may be found in the device from previous use. This value is then divided by the volume of the sampled water to obtain units of dpm/L according to the following equation:

$$A \text{ (dpm/L)} = \frac{S \text{ (cpm)} - BG \text{ (cpm)}}{\varepsilon \cdot V \text{ (L)} \cdot K_i} \dots\dots\dots ^{222}\text{Rn measurements}$$

where:

S : it is the amount of signals from the sample (cpm)

BG (background value): blank measurement (cpm)

ε : it is the efficiency of measurement

V : it is volume of the sample in liters (L)

K_i : decay rate of the nuclide (^{222}Rn)

$$A \text{ (dpm/L)} = \frac{S \text{ (cpm)} - BG \text{ (cpm)}}{\varepsilon \cdot V \text{ (L)} \cdot (1 - K_i)} \dots \dots \dots \text{ } ^{226}\text{Ra measurements}$$

Where $(1 - K_i)$: shows the achieved equilibrium level of radioactive accumulation of ^{222}Rn during incubation period (% of secular equilibrium).

The above two equations for ^{222}Rn and ^{226}Ra measurements return value of activity at the moment of sampling. All samples for ^{222}Rn and ^{226}Ra concentrations were measured and calculated using the same procedure and equations as mentioned above (see Appendix I).

Chapter Six

Results and Discussion

6.1 Results

In addition to the normal components of water hydrogen and oxygen, exist other elements. These elements could be radiogenic elements, organic and inorganic compounds. Radiogenic elements derived from the Uranium and Thorium series could be found in groundwater, these will include ^{226}Ra , ^{224}Ra , ^{223}Ra and ^{222}Rn . Organic compounds in natural water include compounds of low molecular mass such as amino acids, organic acids, while compounds with high molecular mass such humic acid and other anthropogenic organic substances such as oil products, pesticides and polycyclic aromatics. Inorganic compounds are in the form of salts such as calcium, magnesium, potassium, sodium, bicarbonates, carbonates, nitrates, chlorides and sulfates. Table 6.1 and 6.2 present the physical, chemical and radiogenic composition of groundwater in the study area.

Table 6.1: Results of Physical and Radium isotopes measurements

No	Name	Locality	Aquifer	EC (μS/cm)	T ($^{\circ}$ C)	pH	^{226}Ra (Bq/L)	^{222}Rn (Bq/L)	Well Depth(meters)
1	Herodion (1)	Bethlehem	Upper	506	20.2	7.48	0.0086	6.75	350
2	Herodion (2)	Bethlehem	Lower	545	21.8	7.35	0.0237	11.39	770
3	Herodion (3)	Bethlehem	Lower	566	22.8	7.39	0.004	9.7	800
4	Herodion (4)	Bethlehem	Lower	598	24.5	7.28	0.0136	7.15	691
5	PWA I	Bethlehem	Lower	588	20.2	7.33	0.01	2.45	600
6	PWA 11	Bethlehem	Lower	596	21.7	7.28	0.012	7.46	851
7	Izzariya (1)	Bethlehem	Lower	519	26.1	7.46	0.0268	14.58	996
8	Izzariya (2)	Bethlehem	Lower	563	24.1	7.38	0.0173	6.99	793
9	Izzariya (3)	Bethlehem	Lower	629	23.6	7.33	0.037	10.79	835
10	Al Fawar 1	Hebron	Upper	902	20	7.26	0.0055	2.24	100.5
11	Hundaza	Bethlehem	Upper	546	21.9	7.31	0.0168	7.01	330
12	JWC 4	Bethlehem	Lower	513	22.9	7.44	0.0116	8.55	787.5
13	Al Rehea	Hebron	Lower	639	24.9	7.30	0.0332	4.87	495
14	Asamoua	Hebron	Upper	852	21.2	7.32	0.0077	5.02	191

Table 6.2: Results of the chemical analysis in mg/L

No	Name	Na ⁺	K ⁺	Mg ⁺²	Ca ⁺²	NH ₄ ⁺	Cl ⁻	HCO ₃ ⁻	SO ₄ ⁻	NO ₃ ⁻	PO ₄ ⁻	TDS (mg/L)
1	Herodion (1)	44.80	1.27	35.40	88.50	0.01	35.45	489.73	12.00	23.20	0.32	453.0
2	Herodion (2)	9.80	4.61	71.40	62.50	0	30.50	505.65	13.00	6.00	0.06	703.4
3	Herodion (3)	67.60	5.12	10.90	46.70	0.01	30.50	304.70	15.00	5.00	0.08	268.3
4	Herodion (4)	15.25	1.83	11.70	15.60	0.01	30.49	76.44	14.00	13.90	0.36	179.2
5	PWA I	5.70	0.15	31.50	87.20	0.15	33.32	368.65	10.00	16.30	0.11	552.9
6	PWA 11	16.80	2.20	39.00	120.40	0.05	35.45	529.34	13.00	9.00	0.16	765.2
7	Izzariya (1)	15.86	5.84	24.26	57.42	0.01	36.60	251.54	19.00	10.50	0.02	421
8	Izzariya (2)	15.00	2.39	26.80	75.40	0	33.10	327.90	15.00	10.40	0.07	505.9
9	Izzariya (3)	36.90	0.01	36.90	92.20	0.04	51.76	453.16	17.00	21.80	0.31	475.1
10	Al Fawar 1	25.44	14.12	39.68	86.26	0.02	82.95	329.36	45.00	117.50	0.02	740.3
11	Hundaza	13.18	0.67	34.84	65.92	0.01	34.24	336.36	12.00	12.80	0.13	510.0
12	JWC 4	11.68	0.84	28.24	36.36	0.02	33.32	215.92	8.00	17.70	0.11	352.1
13	Al Rehea	33.44	2.61	26.86	84.74	0.02	56.00	366.00	15.00	12.80	0.06	597.5
14	Asamoua	48.74	3.67	25.14	105.94	0	104.60	357.00	32.00	47.60	0.06	725.0

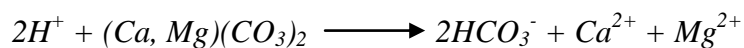
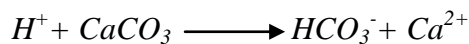
6.2 Water type classification

6.2.1 Piper diagram

The water type in our study were identified by using Piper diagram (Piper, 1944) which is a trilinear plot that permits the classification of water samples into seven water types according to Langguth classification (Langguth, 1966).

According to our results in water chemistry analysis, Piper diagram was plotted by using Aqua Chem (3.7) software. Comparing the two Piper Figures 6.1 and 6.2 shows the majority of the studied wells in Bethlehem- Hebron districts are characterized in one main group with normal earth alkaline water with prevailing bicarbonate. Three wells (Asamoua, Herodion 3 and Herodion 4) are characterized in another group mainly earth alkaline water with increased portions of alkalis with prevailing bicarbonate.

This type of the main water group could be due to natural processes that had happen in the carbonate aquifer such as the dissolution of carbon dioxide (CO_2) from the atmosphere and from the soil horizon that causes the dissolution of the carbonate minerals, calcite $CaCO_3$ and dolomite $Ca,Mg(CO_3)_2$. The following reactions that describe the geochemical processes:



That explains the high concentration of the anion HCO_3^- as well as the high concentration of the cation Ca^{2+} and Mg^{2+} in the majority of the wells in the aquifer.

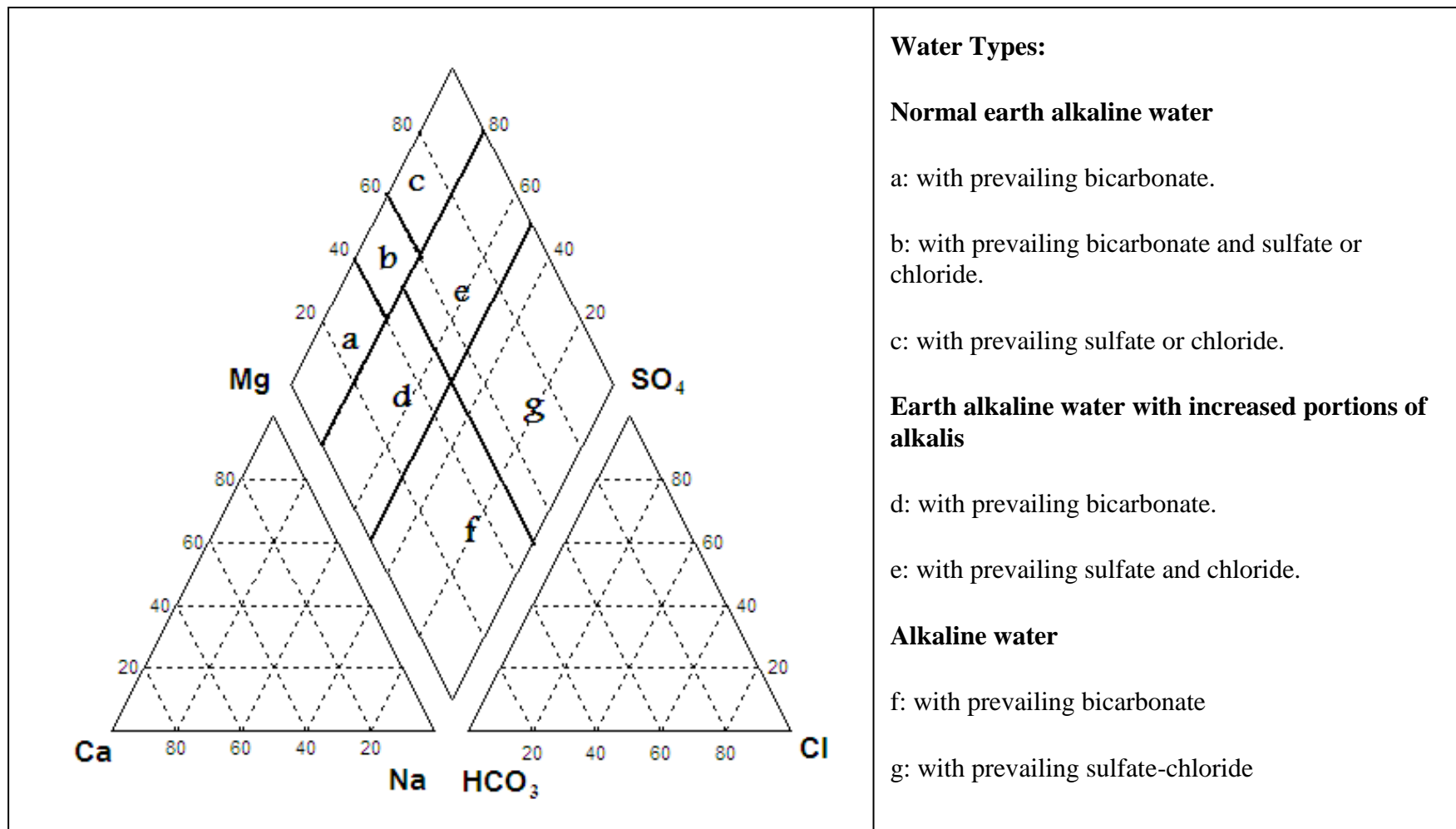


Figure 6.1: Piper trilinear diagram with classification of water types (Langguth, 1966).

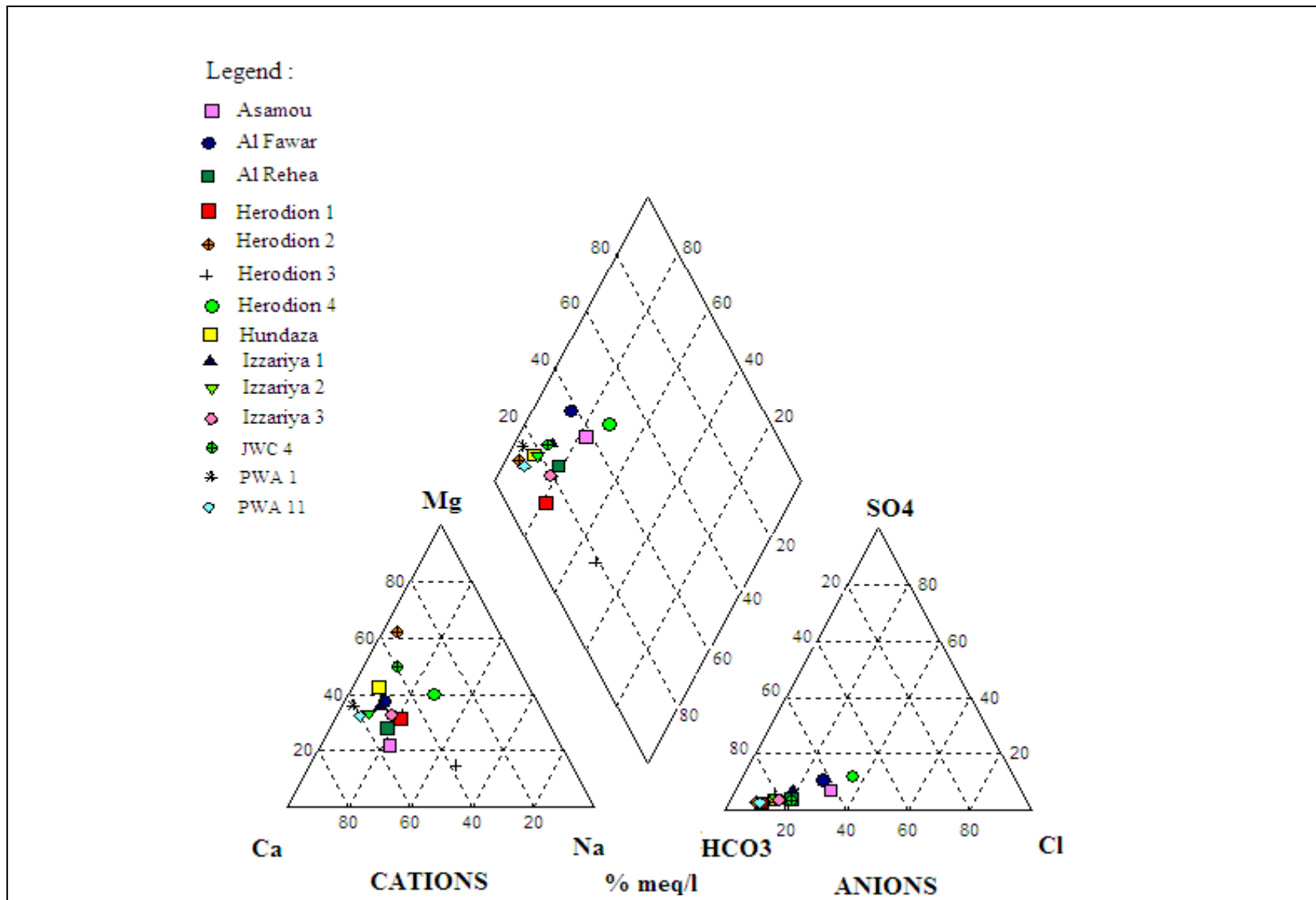


Figure 6.2: Piper diagram showing the wells studied in Bethlehem-Hebron districts

6.3 Saturation Indices

Saturation indices are a method for expressing the extent of chemical equilibrium between the mineral phases of the aquifer materials and water. The major key factor in the chemistry of groundwater is the interaction of recharge water with soil and rocks. These interactions are mainly precipitation and dissolution processes and both are controlled by the solubility products of the different mineral phases. In general, the saturation indices (SI) are used to express the tendency of water towards precipitation or dissolution of certain mineral phases (Al Kuisi, 1998). Through the calculations of the saturation index, we can determine the equilibrium state of water with a mineral phase in the matrix.

The equation that represents the degree of water saturation with respect to a certain mineral is :

$$SI = \log (K_{IAP} / K_{SP}) \quad \text{where}$$

SI : is the saturation index of the particular mineral

K_{IAP} : is the ion activity product of the ions

K_{SP} : is the solubility product of the mineral

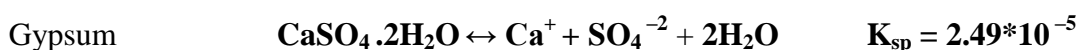
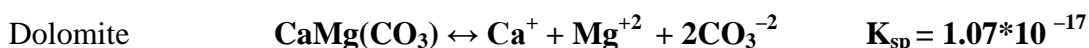
The importance of the saturation indices is to reveal the possible dissolution / precipitation processes during the water-rock interaction. The value of the saturation index is interpreted below:

SI value = 0: This means that the water is in equilibrium with respect to the particular mineral.

SI value < 0: This means that the water is undersaturated with respect to that mineral and tends towards its dissolution.

SI value > 0: This means that the water is oversaturated with respect to that mineral and tends towards its precipitation.

The minerals considered in the calculation, with their essential thermodynamic data are illustrated in the following equations:



By using Aqua Chem software (3.7) through PHREEQC we had calculated the saturation indices of calcite, dolomite and gypsum for the studied wells as shown in Table 6.3.

Table 6.3: Saturation Indices of the wells studied in Bethlehem–Hebron districts with respect to calcite, dolomite and gypsum minerals.

Name	Saturation Index (SI)			
	Calcite	Dolomite	Gypsum	Aquifer
Al Fawar (1)	0.12	0.18	-1.95	Upper
Asamoua	0.32	0.32	-2.00	Upper
Hundaza	0.12	0.28	-2.58	Upper
Herodion (1)	0.53	0.94	-2.50	Upper
Al Rehea	0.29	0.43	-2.40	Lower
PWA(1)	0.27	0.39	-2.55	Lower
Herodion (4)	-1.04	-1.87	-2.94	Lower
Herodion (2)	0.27	0.92	-2.65	Lower
Izzariya (2)	0.27	0.44	-2.42	Lower
JWC (4)	-0.14	-0.07	-2.94	Lower
Herodion (3)	0.05	-0.22	-2.56	Lower
Izzariya (3)	0.41	0.75	-2.34	Lower
PWA (11)	0.50	0.82	-2.55	Lower
Izzariya (1)	0.16	0.32	-2.40	Lower

The results in Table 6.3 show that all groundwater samples were undersaturated with respect to gypsum and they tend towards dissolution. While almost all the groundwater samples were found to be oversaturated with respect to calcite and dolomite and thus tend towards precipitation. Samples taken from Herodion 4, and JWC 4 were found to be undersaturated with respect to calcite and dolomite while Herodion 3 is undersaturated with respect to dolomite only.

6.4 Radium isotopes analysis in the Upper and Lower Cenomanian Aquifers

The evaluation of radiogenic components and the chemical constituents of the groundwater flows by the three major components which are; aquifer system location (Upper–Lower), recharge and discharge and well depth.

Table 6.4: Radium, Radon concentration, Total Hardness and well depth of the study area.

Well Name	Aquifer	EC ($\mu\text{S/cm}$)	^{226}Ra (Bq/L)	^{222}Rn (Bq/L)	$^{226}\text{Ra}/^{222}\text{Rn}$	Well depth (meters)	Total Hardness (mg/L CaCO_3)
Al Fawar (1)	Upper	902	0.0055	2.24	0.0076	100.5	378.4
Asamoua	Upper	852	0.0077	5.02	0.0015	191	367.7
Hundaza	Upper	546	0.0168	7.01	0.0024	330	307.8
Herodion (1)	Upper	506	0.0086	6.75	0.0013	350	366.4
Al Rehea	Lower	639	0.0332	4.87	0.0068	495	321.9
PWA 1	Lower	588	0.012	2.45	0.0041	600	347.1
Herodion (4)	Lower	598	0.0136	7.15	0.0019	691	87.1
Herodion (2)	Lower	545	0.0237	11.39	0.0021	770	449.6
Izzariya (2)	Lower	563	0.0173	6.99	0.0025	793	298.4
JWC 4	Lower	513	0.0116	8.55	0.0014	787.5	206.9
Herodion (3)	Lower	566	0.004	9.7	0.0004	800	161.4
Izzariya (3)	Lower	629	0.037	10.79	0.0034	835	381.8
PWA 11	Lower	596	0.012	7.46	0.0016	851	460.8
Izzariya (1)	Lower	519	0.0268	14.58	0.0018	996	243.1

6.4.1 Upper Cenomanian–Turonian Aquifer:

The Upper Cenomanian–Turonian Aquifer is composed of Jerusalem, Bethlehem and Hebron Formation, its total thickness varies between 350–370m. The lithology of Jerusalem and Hebron Formation are nearly the same and are composed of karstic limestone and dolomite as an aquifer. Bethlehem Formation is composed of chalky limestone and marl as an aquitard and hard gray porous dolomite as an aquifer. In order to understand some interactions such as the nuclear alpha–particle recoil and chemical processes, such as ion exchange, sorption and precipitation; two major factors were to be considered such as the role of aquifer solids in controlling the radionuclides behavior in water and their total solution composition in the water (Oliveira, et al., 1998).

6.4.1.1 Upper Cenomanian Aquifer – Well depth and Electrical Conductivity (EC):

Four wells with depth ranging between 100.5 m and 350 m abstracting water from the Upper aquifer. The electrical conductivities of water range between 506 and 902 $\mu\text{S}/\text{cm}$, the highest value was recorded in Al Fawar well (1). Figure 6.3 shows a strong negative correlation ($r= 0.97$) between well depth and electrical conductivity. This could be due to the dissolution of sulfate and nitrate that are used in agriculture soil that increase the electrical conductivity at low depth wells in the Upper Aquifer as demonstrated in Tables 6.2 and 6.5. Both Al Fawar (1) (100.5 m) and Asamoua (191 m) wells had the highest concentration of both sulfate and nitrate ions with the highest electrical conductivity. Comparing to the low electrical conductivity of the rainfall that was measured with an average of 159.78 $\mu\text{S}/\text{cm}$ (Qabajeh, 2008).

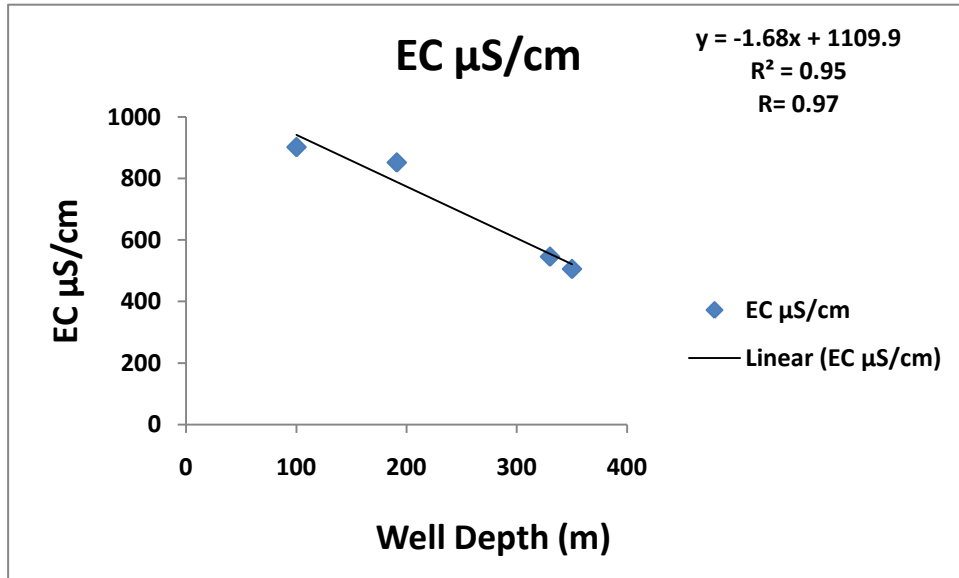


Figure 6.3: Negative linear correlation between well depth and Electrical Conductivity in the Upper Aquifer.

6.4.1.2 Upper Cenomanian Aquifer– Well depth and sulphate concentration (SO_4^{-2}):

Sulfate concentration range between 12 and 45 mg/L, where the highest value was recorded at depth of 100.5 m well (Al Fawar 1). A strong negative correlation between well depth and sulphate concentration with $r = 0.99$ is shown in Figure 6.4.

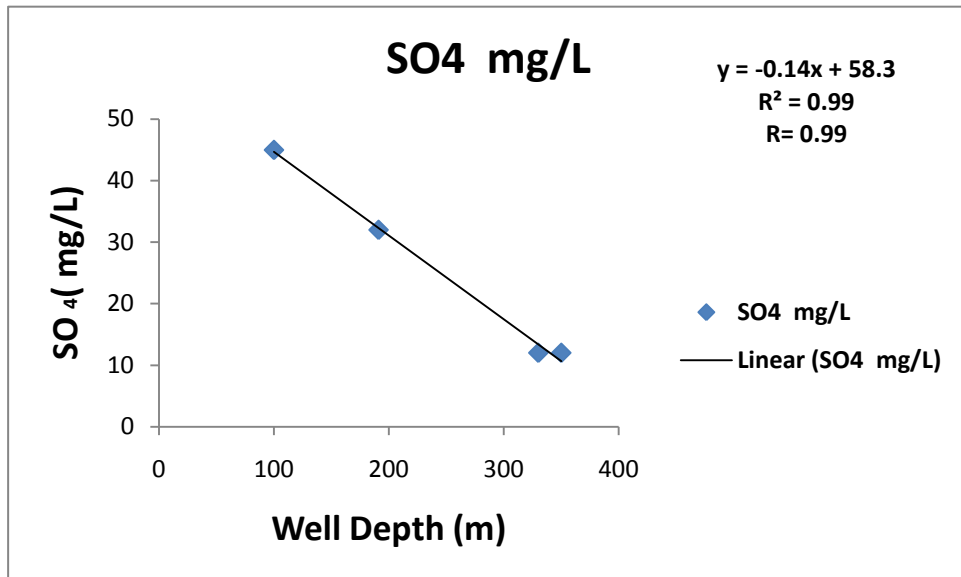


Figure 6.4: Negative linear correlation between well depth and sulphate concentration in the Upper Aquifer.

6.4.1.3 Upper Cenomanian Aquifer– Well depth and nitrate concentration (NO₃⁻):

Nitrate concentration range between 12.8 and 117.5 mg/L, where the highest value was recorded at depth of 100.5 m well (Al Fawar 1), this indicate that the source of NO₃⁻ is due to the fertilizers used in agriculture. A negative correlation with $r = 0.93$ was found with depth as shown in Figure 6.5.

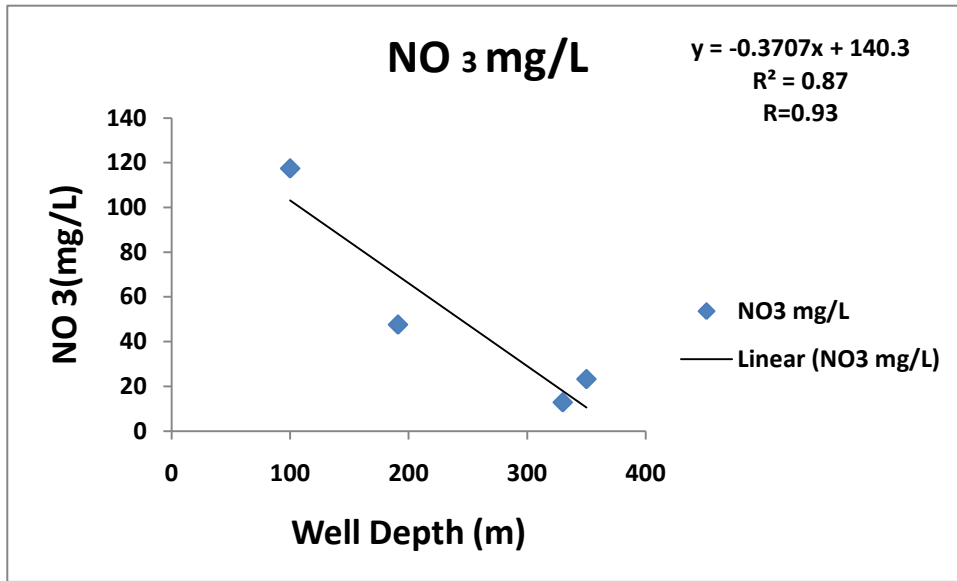


Figure 6.5: Negative linear correlation between well depth and nitrate concentration in the Upper Aquifer.

6.4.1.4 Upper Cenomanian Aquifer – Well depth and Radon concentration (²²²Rn):

Radon concentration range between 2.24 Bq/l in Al Fawar (1) well and increase eastwards to 6.75 Bq/l in the Herodion (1) well. Figure 6.6 shows a strong positive correlation between depth increase and ²²²Rn concentration with $r = 0.97$. This could be due to the increase contact time between water and radioactive bearing minerals. The greater depth of the well allows more water to interact with greater thickness of the aquifer (Choubey, et al., 2003).

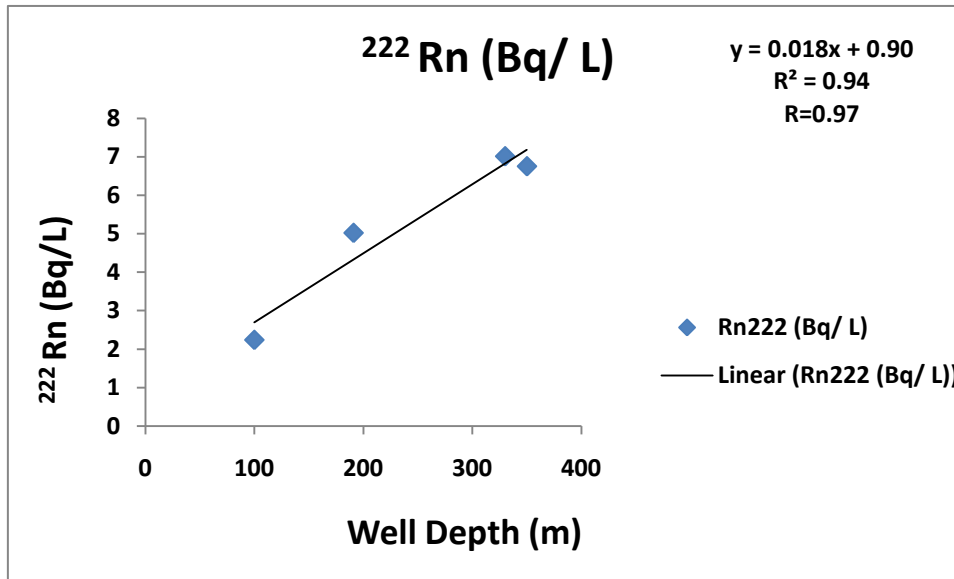


Figure 6.6: Positive linear correlation between well depth and ^{222}Rn concentration in the Upper Aquifer

6.4.1.5 Upper Cenomanian Aquifer – Well depth and $^{226}\text{Ra}/^{222}\text{Rn}$ ratio:

The Radium contents range between 0.004 Bq/l and 0.0136 Bq/l. The low $^{226}\text{Ra}/^{222}\text{Rn}$ ratio in groundwater indicate that the ^{226}Ra is not mobile in water and that ^{226}Ra is probably connected to iron and manganese oxide of the soil forming minerals that is found in the carbonate aquifer, while ^{222}Rn diffused into the water from the rock (Hassan, 2008). As illustrated in Figure 6.7 with a coefficient correlation ($r = 0.84$).

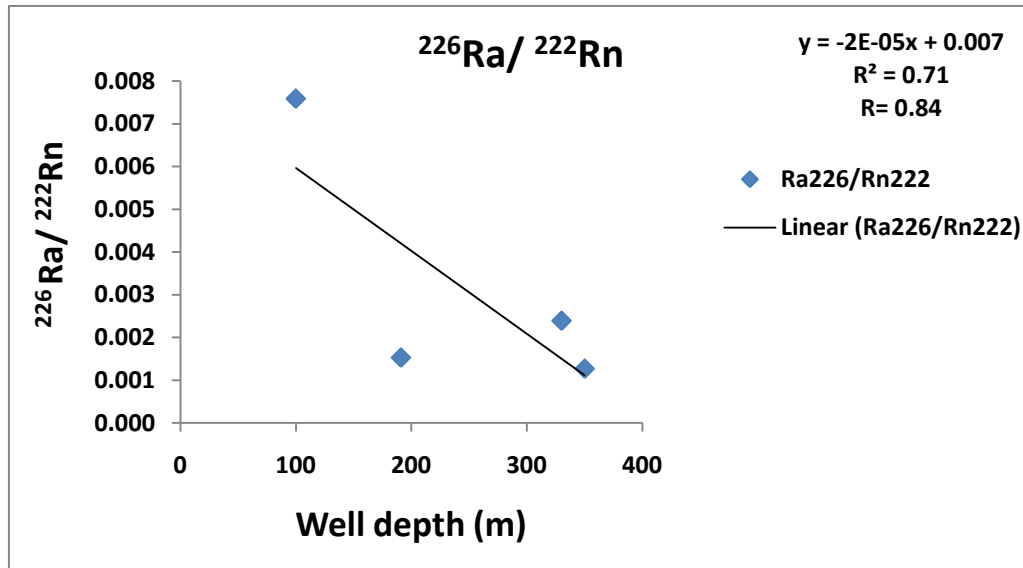


Figure 6.7: Negative linear correlation between well depth and $^{226}\text{Ra}/^{222}\text{Rn}$ ratio in the Upper Aquifer.

6.4.1.6 Upper Cenomanian Aquifer–Saturation Index (calcite) with ^{226}Ra concentration:

The important chemical reactions are those of adsorption of Radium to active surfaces of all kinds and co-precipitation with Ca^{+2} salts in particular (Oliveira, et al., 1998). Calcite saturation indices is very important to present the geochemical conditions of water. If water is saturated with respect to calcite, then it will precipitate. There is a possibility that the increase in the saturation indices of calcite lead to the removal of Ca^{+2} from the solution by precipitation and the decrease in ^{226}Ra concentration could be ascribed to the adsorption of ^{226}Ra on the active surfaces of Ca^{+2} and then co-precipitate with Ca^{+2} in some of the studied wells. Figure 6.8 illustrates this negative relation with coefficient correlation $r = 0.86$ in the Upper Aquifer.

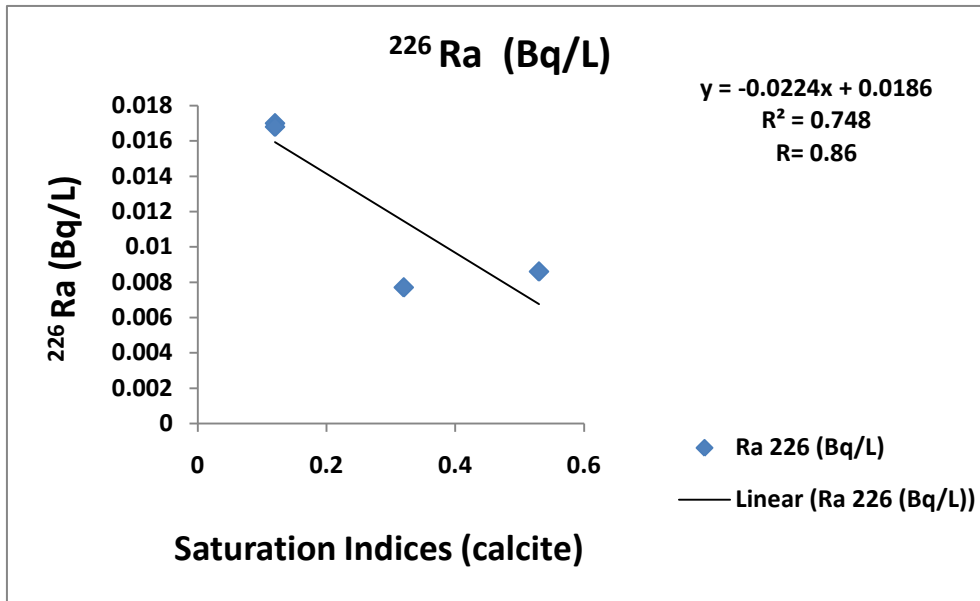


Figure 6.8: Negative linear correlation between Saturation Indices (calcite) and ²²⁶Ra concentration in the Upper Aquifer.

In studying the relation between the total hardness (mg/L CaCO₃) of the water with the concentration of ²²⁶Ra, a negative linear correlation with ($r= 0.99$) is illustrated in Figure 6.9. This indicates as total hardness increases this will lead to the increase the possibility of precipitation of calcite thus lead to decrease the ²²⁶Ra concentration as it will co precipitate with the calcite.

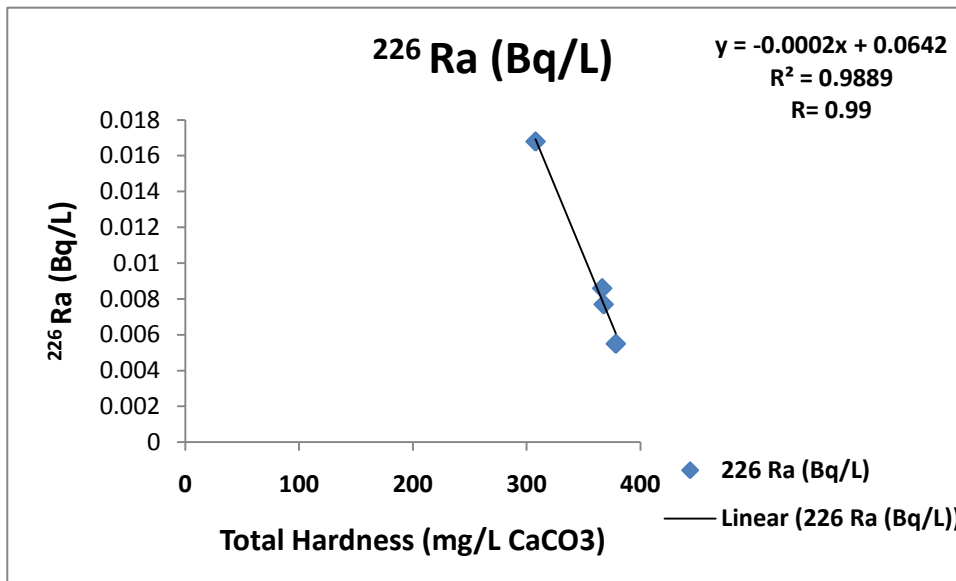


Figure 6.9: Negative linear correlation between Total Hardness (mg/L CaCO₃) and ²²⁶Ra concentration in the Upper Aquifer.

6.4.2 Middle Cenomanian Aquiclude:

The Middle Cenomanian aquiclude is composed of Yatta Formation. The lithology of this aquiclude that separates the Upper and the Lower Cenomanian is composed of bluish–greenish clay, marl and chalk (Guttman & Zuckerman, 1995 and Guttman et al., 2000). The total thickness of this aquitard varies between 150–200m. The separation is manifested in the difference in water levels in the two sub–aquifers. The groundwater levels in the upper aquifer are higher than those in the lower aquifer throughout most of the area (Guttman & Zuckerman, 1995 and Guttman et al., 2000).

6.4.3 Lower Cenomanian Aquifer:

The Lower Cenomanian Aquifer is composed of Upper and Lower Beit Kahil Formations. Its total thickness varies between 300–320 m. The lithology of these formations consist of limestone and dolomite inter–bedded with marl as well as limestone , dolomite and marly

limestone. The high water bearing capacity and productivity is owed to the great thickness of the carbonates, mainly dolomitic limestone and limestone (Hasan, 2008).

6.4.3.1. Lower Cenomanian Aquifer – Well depth and Electrical Conductivity (EC):

Ten wells with well depth ranging from 495 m to 996 m abstracting water from the Lower Aquifer. The electrical conductivities of water ranges from 513 to 639 $\mu\text{S}/\text{cm}$ which is considered as one group due to its narrow range. The highest EC was recorded in Al Rehea well 495 m in depth; a negative correlation with $r = 0.58$ is shown in Figure 6.10.

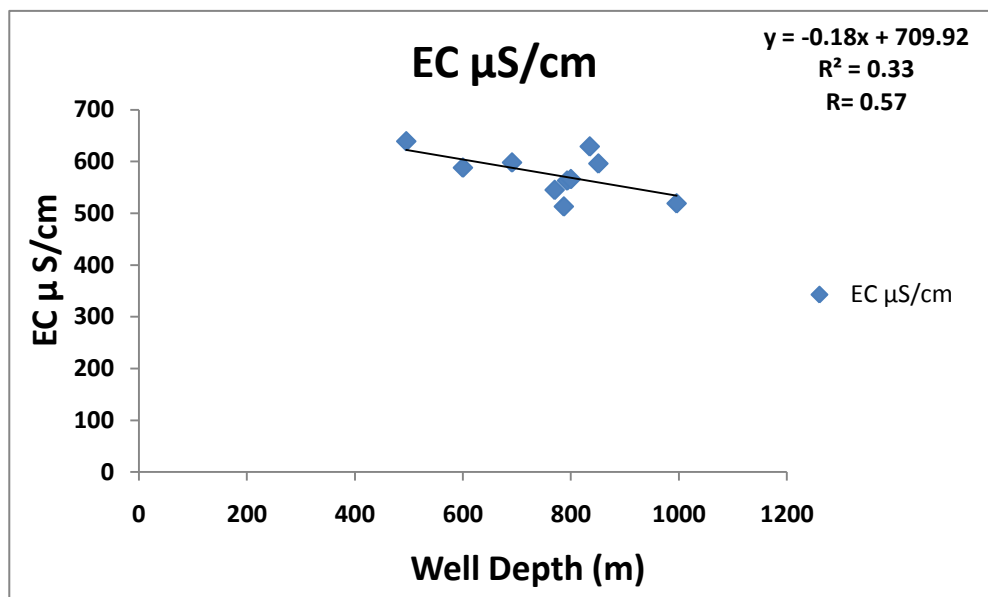


Figure 6.10: Negative linear correlation between well depth and Electrical Conductivity in the Lower Aquifer.

6.4.3.2 Lower Cenomanian Aquifer – Well depth and Radon concentration (^{222}Rn):

In the lower Aquifer ^{222}Rn concentration ranges from 2.45 Bq/L in PWA (1) to 14.58 Bq/L in Izzariya (1). The ^{222}Rn concentration in the Lower Aquifer is higher than in the Upper Aquifer as the Lower Aquifer is considered as a confined aquifer and ^{222}Rn remain trapped in the water. Figure 6.11 shows positive correlation between depth increase and ^{222}Rn concentration with $r = 0.83$.

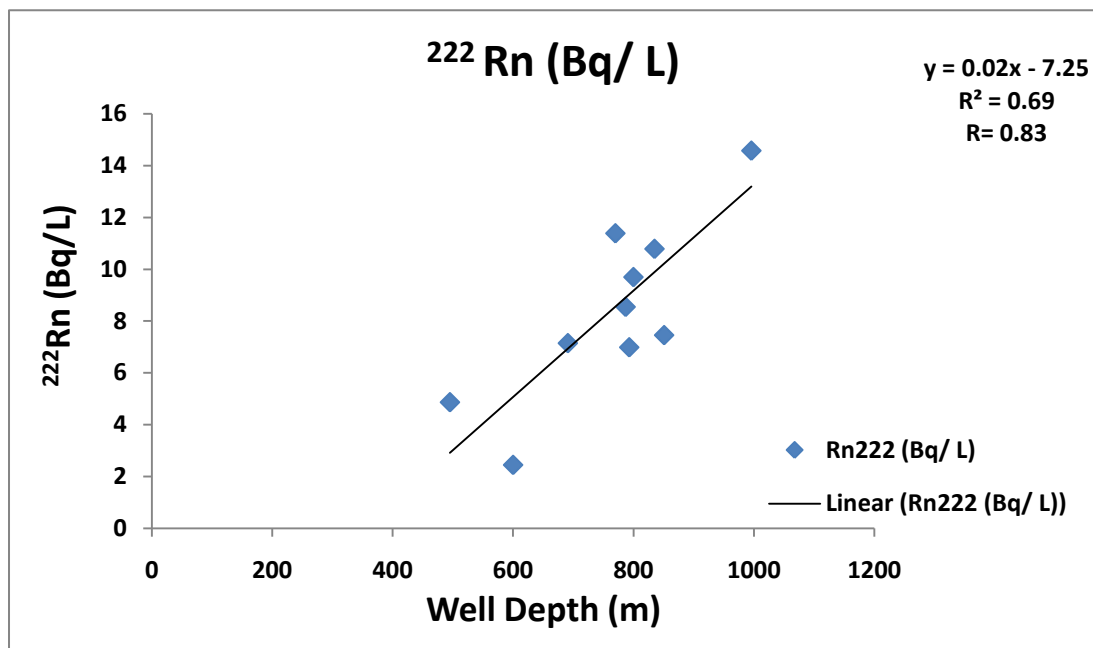


Figure 6.11: Positive linear correlation between well depth and ^{222}Rn concentration in the Lower Aquifer

6.4.3.3 Lower Cenomanian Aquifer – Well depth and $^{226}\text{Ra}/^{222}\text{Rn}$ ratio

The Radium concentration ranges from 0.0004 Bq/l to 0.0068 Bq/l. The decrease in the ratio $^{226}\text{Ra}/^{222}\text{Rn}$ with the well depth in the lower Aquifer with $r = 0.8$ as shown in figure 6.12 appears that the transport of Radium by groundwater may be extremely limited owing to continual exchange with the aquifer solids. While it has been observed that the escape of Radon occurs mainly through direct recoil and diffusion (Oliveira, et al., 1998).

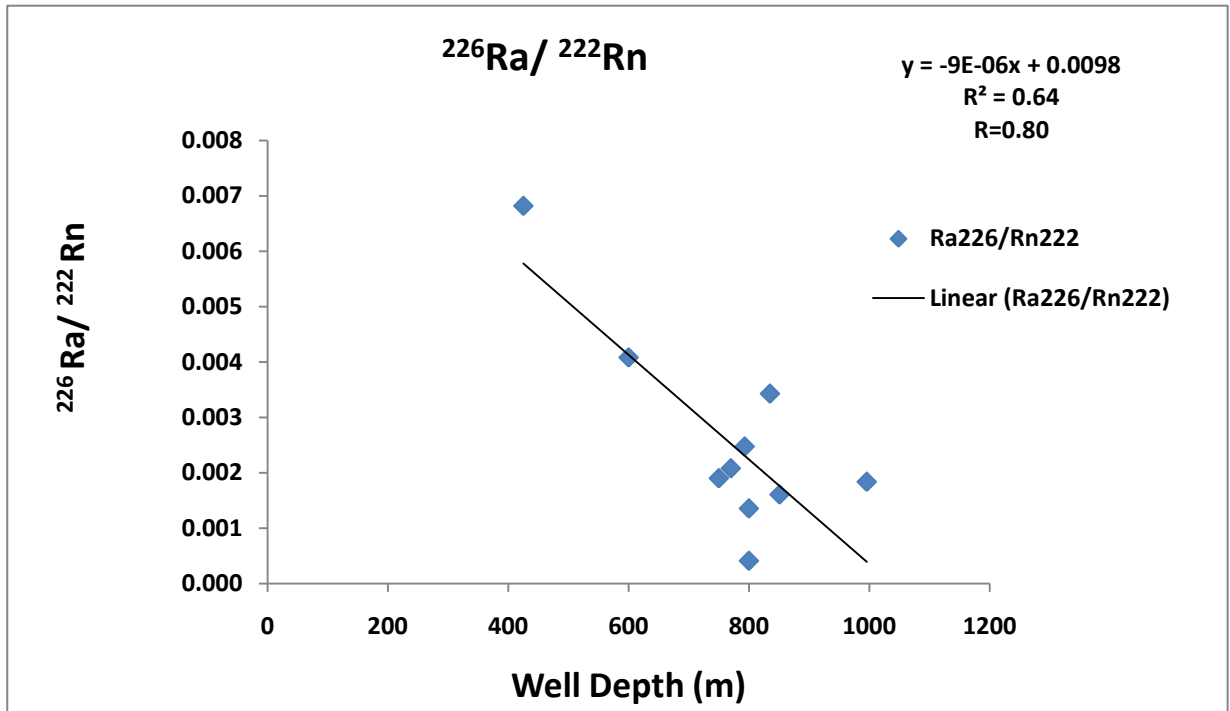


Figure 6.12: Negative linear correlation between well depth and $^{226}\text{Ra}/^{222}\text{Rn}$ ratio in the Lower Aquifer.

6.4.4 Data interpretation for Upper and Lower Cenomanian Aquifers:

6.4.4.1 Well depth and ^{222}Rn concentration in Upper and Lower Aquifers

In combining both data from Upper and Lower Cenomanian Aquifer in relation to well depth and ^{222}Rn concentration Figure 6.13 illustrates the correlation between the two variables with coefficient correlation $r = 0.74$

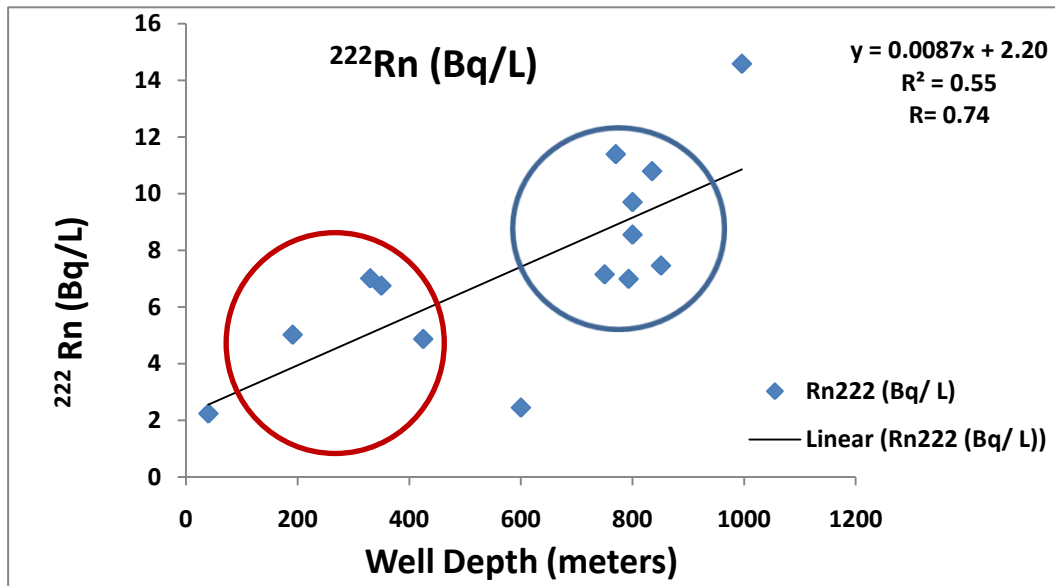


Figure 6.13: Positive Linear correlation between well depth and ²²²Rn concentration of the Upper Aquifer –red circle– and the Lower Aquifer– blue circle.

6.4.4.2 Correlation between ²²²Rn , ²²⁶Ra concentration and distance from West to East

According to the wells going from West to East there is an increase in the ²²²Rn concentration with a good positive correlation with $r = 0.7$ as illustrated in Figure 6.14. While there is no trend between the ²²⁶Ra concentrations with the distance going from West to East as illustrated in Figure 6.15. According to our results we can conclude that the ²²²Rn concentration is much higher than the ²²⁶Ra concentration in the Cenomanian Aquifer as we are going from West to East in the Southern part of the West Bank. This could be ascribed to the increasing of faults while going from West to East in the studied area in the Mountain Aquifer as shown in Figure 6.16.

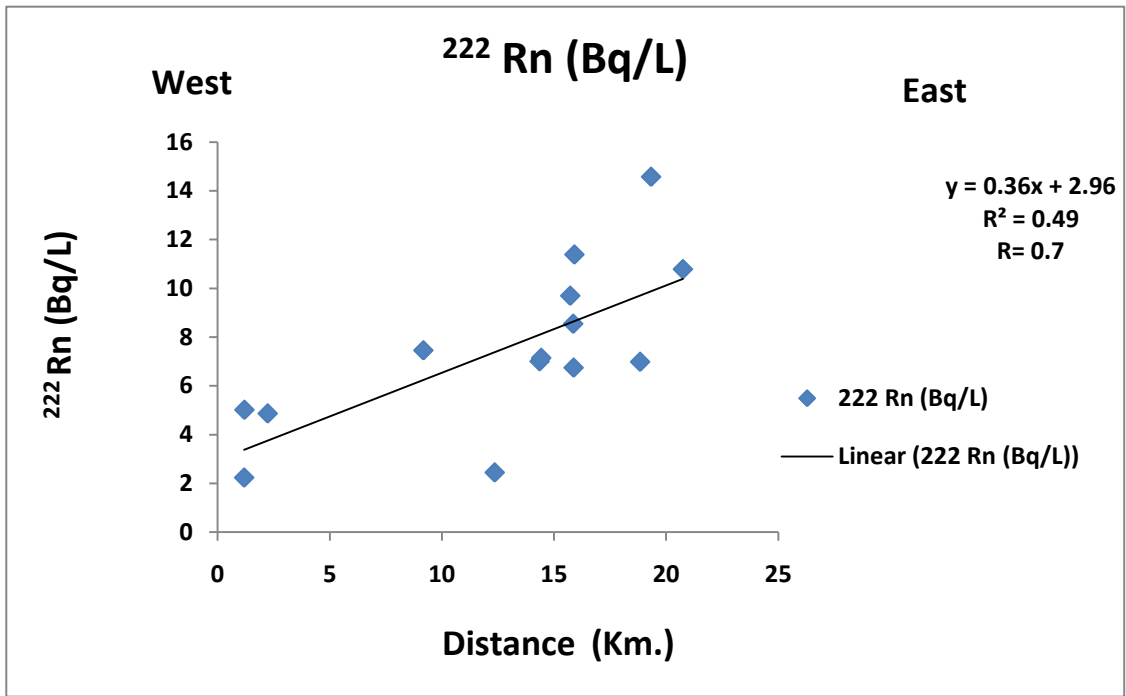


Figure 6.14: Positive Linear correlation between the distance to the East and ^{222}Rn concentration.

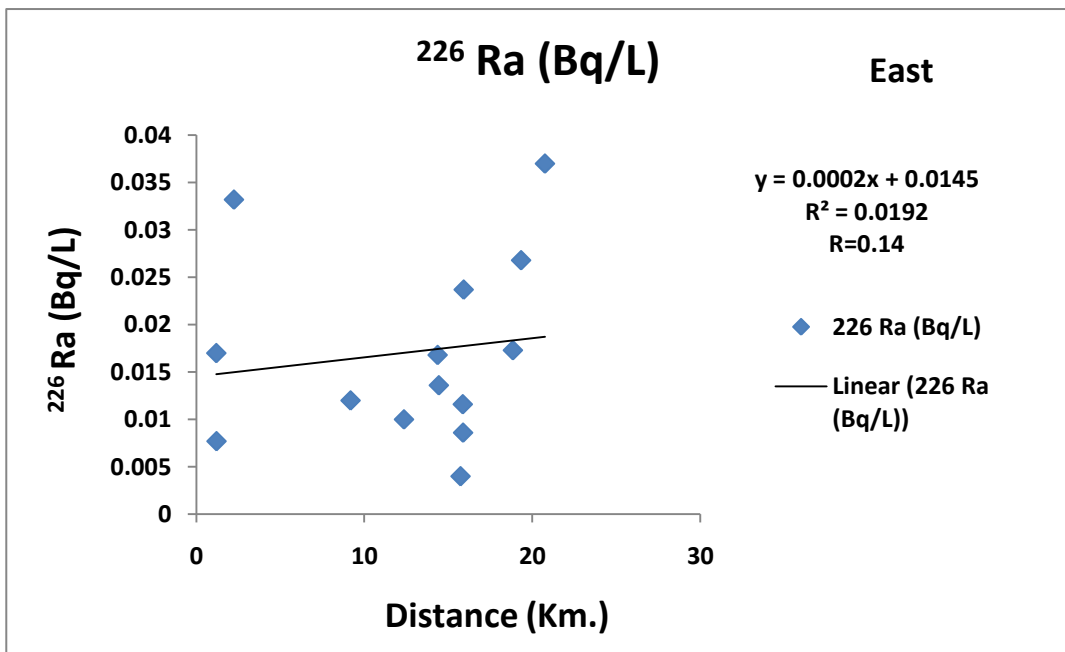


Figure 6.15: No trend between the distance to the East and ^{226}Ra concentration.

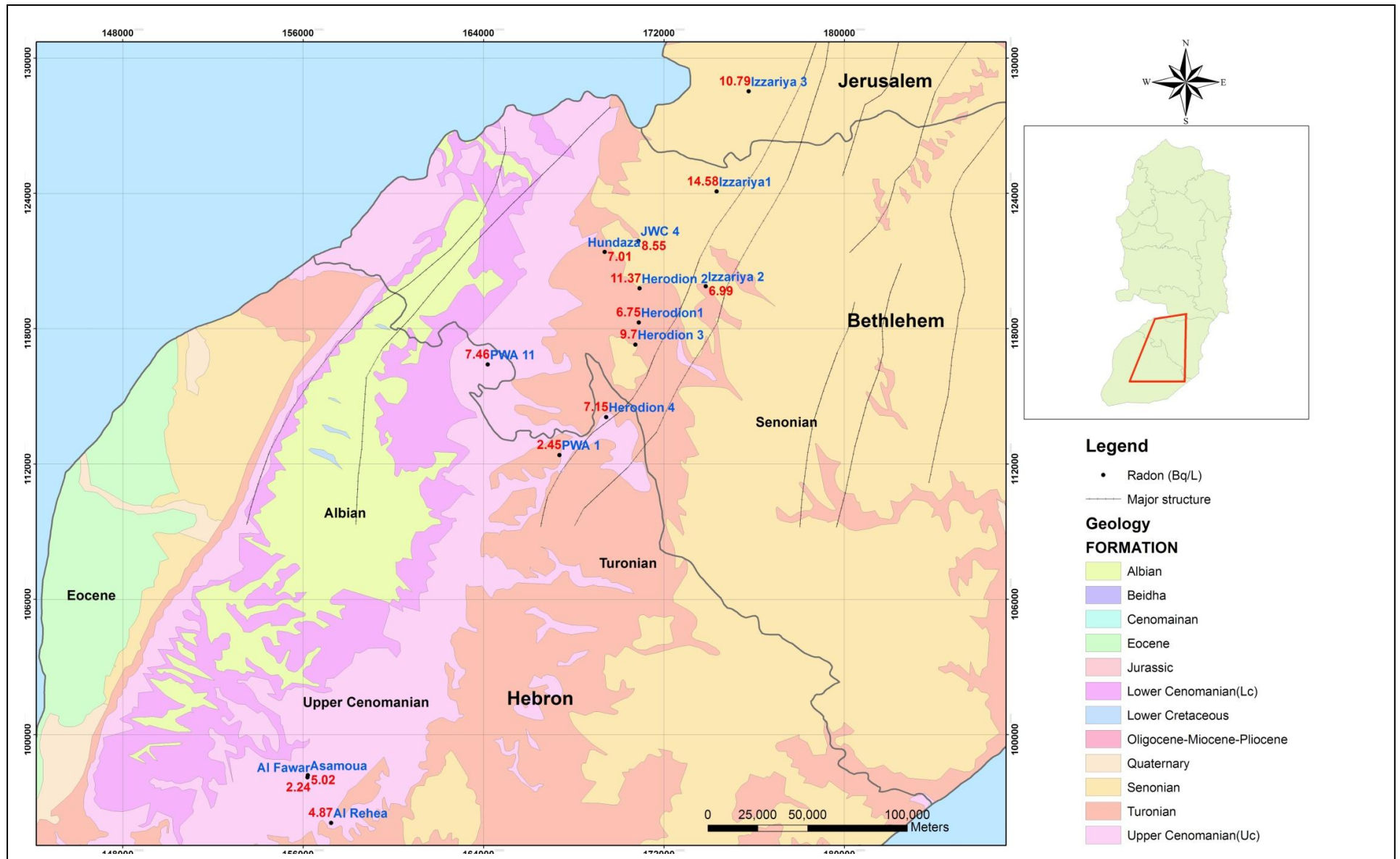


Figure 6.16: Location of the studied wells in relation to the ^{222}Rn concentration and the faults from West to East in Bethlehem-Hebron districts.

6.5 Summary of the results

According to our data we can summarize our results in this study in the following points:

- Referring to the water type classification, we can classify our data by using the Piper Diagram that most of the studied wells belong to one main group with normal earth alkaline water with prevailing bicarbonate ($\text{Ca}^{+2}, \text{Mg}^{+}, \text{HCO}_3^{-}$) which is the characteristics of the carbonate aquifer. Analyzing our data by using Durov Diagram we can conclude that the dominant ions are HCO_3^{-} and Ca^{+2} which are typical for recharging water in limestone.
- In the Upper Cenomanian Aquifer a negative correlation was revealed between the well depth and the electrical conductivity. Both nitrate and sulphate concentrations were high at low well depth due to the contamination and the usage of fertilizers at the surface of the topsoil. No correlation was observed between electrical conductivity and ^{226}Ra and ^{222}Rn concentration in the studied wells.
- In both Upper and Lower Cenomanian Aquifer a very good positive correlation was indicated between well depth and ^{222}Rn concentration due to that more water will interact with greater thickness of the aquifer. While a negative correlation was observed between the $^{226}\text{Ra}/^{222}\text{Rn}$ ratio and the well depth in the studied wells in Bethlehem–Hebron districts.
- Most of the groundwater in the studied wells in both Upper and Lower Cenomanian Aquifer was oversaturated with respect to calcite and dolomite and thus the minerals tend towards precipitation. The relation between the ^{226}Ra concentration and the saturation indices of calcite is highly negative in the Upper Aquifer with $r = 0.86$ leading to the possibility of co-precipitation of ^{226}Ra with Ca^{+2} salts in the studied wells in Bethlehem–Hebron districts in the Upper Aquifer thus leading to

the low concentration of ^{226}Ra (0.0077 Bq/L–0.017 Bq/L) over the ^{222}Rn concentration (2.24 Bq/L–6.75Bq/L) . These results were confirmed by studying the relation between the Total Hardness of water and the ^{226}Ra concentration leading to a highly negative correlation coefficient ($r= 0.99$).

- As a result water going from the recharge area at Hebron mountains in the West to the discharge area in the East, ^{222}Rn concentration will increase with a coefficient correlation of $r=0.7$ while no relation with ^{226}Ra concentration was observed. This could be ascribed to the increasing of faults while going from West to East in the studied area.

6.6 Conclusions

In general the radionuclides in each decay series are generally expected to be in secular equilibrium and so have equal activities. In contrast, these nuclides especially in our study ^{226}Ra and ^{222}Rn exhibit relative fractionations within the surrounding groundwater that reflect contrasting behavior during release into the water and during interaction with the surrounding host aquifer rocks .

In general the earth alkaline Radium is readily removed from groundwater by water-rocks interactions and is strongly depleted, comparing to the high activities of the ^{222}Rn which reflects the lack of reactivity of this noble gas without the complications of removal by adsorption or precipitation.

The observation of variations of Radium and Radon concentrations in groundwater supplies suggested that the scale length of ^{222}Rn migration in groundwater transport may be greater than that of ^{226}Ra , despite the much longer half-life of ^{226}Ra . It appears that the

transport of Radium by groundwater may be extreme limited owing to continual exchange with the aquifer solids.

6.7 Recommendations:

In addition to the results and conclusions that had been discussed several recommendations could be taken into considerations:

- A general survey of radioactivity in water must be conducted in the West bank through the Palestinian Water Authority, and the results must be compared with the Environmental Protection Agency guideline levels. Drinking water should be controlled for radioactive contaminants and appropriate measures should be taken if the activity detected exceeds the permissible levels.
- Several factors that control the concentration of radium in the groundwater could be studied such as: groundwater flow direction and velocity, groundwater residence time in the aquifer, concentration of other chemical elements such as Ba due to its similarity of chemical properties to Ra.
- Further investigations for Radium concentration must be studied in soil.

References:

- Abdul-Jaber, Q., Abed Rabbo, A., Scarpa, D., Qannam, Z., Younger, P., (1999). **Wells in the West Bank: Water Quality and Chemistry.**
- Air & Water Quality Inc. (2000).” ***The Problem Solvers*”. Radon in your Water.**
http://www.awqinc.com/radon_water.html (29/05/2009)
- Alabdula’aly, A.I. (1999). ***Occurrence of Radon in the Central Region Groundwater of Saudi Arabia.*** Journal of Environmental Radioactivity, 44, 85-95.
- Al Kuisi, M., (1998). ***Effects of irrigation water with special regards on soil and groundwater in the Jordan Valley area / Jordan,*** PhD. Thesis, Munstersche forschungen zur geologie and palaontologie.
- Almeida, R.M.R., Lauria, D.C., Ferreira, A.C., Sracek, O. (2004). ***Groundwater radon, radium and uranium concentrations in Regiao dos Lagos, Rio de Janeiro State, Brazil.*** Journal of Environmental Radioactivity, 73, 323-334.
- Annunziata, F.M. (2003). ***Handbook of radioactivity analysis,*** 2nd edition. USA: Academic Press.
- Asikainen, M. (1981). ***State of disequilibrium between ^{238}U , ^{234}U , ^{226}Ra and ^{222}Rn in groundwater from bedrock.*** Geochimica et Cosmochimica Acta, 45, 201-206.
- CDM / Morganti– Assisting organization (1997): ***Two stage well development study for additional supplies in the West Bank.*** Palestinian Water Authority–water resources Program (unpublished report).
- Charles, M. (2001). UNESCAR Report 2000: ***Sources and Effects of Ionizing Radiation.*** Journal of Radiological Protection.21 (1), 83-85.
- Choubey, V.M., Bartarya, S.K., Ramola, R.C. (2003). ***Radon in groundwater of eastern Doon valley, Outer Himalaya.*** Radiation Measurements, 36, 401-405.
- Clark, I.D. and Fritz, P. (1997): ***Environmental isotopes in hydrogeology.*** Lewis Publishers, New York.
- Copenhaver, S.A., Krishnaswami, S., Turekian, K.K., Epler, N., Cochran, J.K. (1993). ***Retardation of ^{238}U and ^{232}Th decay chain radionuclides in Lond Island and Connecticut aquifers.*** Geochimica Cosmochimica Acta, 57, 597-603.

- Defra, (1999). *Radioactivity and Environmental Protection*. U.K.

<http://www.defra.gov.uk/environment/radioactivity/background/> (28/05/2009)
- Degrémont, S., (1991): *Water Treatment Handbook*. 6th edition. Lavoisier Publishing, France.
- Dickson, B. L. (1985). *Radium isotopes in saline seepages, south-western Yilgran, Western Australia*. *Geochimica Cosmochimica Acta*, 49, 361-368.
- Dickson, B. L. (1990). *Radium in Groundwater*. Commonwealth Scientific and Industrial Research Organization, Australia.
- Dickson, B.L.& Herczeg, A.L. (1991). *Naturally-occurring radionuclides in acid-saline groundwaters around Lake Tyrrell, Victoria, Australia*. *Chemical Geology*, 96, 95-114.
- Durrige Company Inc. (2001). *RAD7 RAD-H₂O: Radon in Water accessory*. Owner's Manual.
- Eisenbud M., Gesell T. (1997). *Environmental Radioactivity: from natural, industrial and military sources*. 4th edition, Academic press, San Diego.
- Environmental Protection Agency (EPA). (2000). **Radiological aspects**.
- Giffin, C., Kaufman, A., Broecker, W.S., 1963. *Delayed coincidence counter for the assay of action and thoron*. *J. Geophys.Res.* 68, 1749-1757.
- Grainger, R.C., (1986). *Some Factors Affecting the Distribution of Radon*. *The Journal of the Royal Society for the Promotion of Health*, 100-101.
- Guttman, J. and Zuckerman, CH. (1995). *A model of the flow in the Eastern Basin of the Mountains of Judea and Samaria from the Far'ah to the Judean Desert*. Water Planning for Israel, Inc (Tahal), Tel Aviv. (unpublished report).
- Guttman, J., Flexer, A., Hoetzi, H., Ali, W., Bensabat, J., and Yellin-Dror, A., 2000. *Hydrogeology of the eastern aquifer in Judea hills and Jordan Valley*. German-Israeli-Palestinian Joint Research. Mekorot Report 468. Project 02WT9719.
- Guy, S., (1988). *An overview of Natural Background Radiation Sources, Part 1: External Sources of Radiation Exposure*. Alara Consultanta cc, U.S.A.
- Gvirtzman, H., (1994). *Ground water Allocation in Judea and Samaria, In: Water and Peace in the Middle East*. Issac, J. and Shuval, H., Elsevier, Amsterdam.

- Hassan, J., (2008). *Hydrogeology and Hydrochemistry of the brackish Ein Feshcha Spring Group (Dead Sea area)*. Ph.D thesis University of Karlsruhe, Germany. 113-126.
- Human Health Fact Sheet (2005). *Natural Decay Series: Uranium, Radium, and Thorium*. Argonne National Laboratory, EVS.
<http://www.ead.anl.gov/pub/doc/natural-decay-series.pdf>, (26.05.2009)
- Issar, A.S. (1993): *Salination processes in the carbonate aquifers in Israel*. Environmental Geology, 21: 152-159.
- Jacomino, V.F., Bellintani, S.A., Oliveira, J., Mazzilli, B.P., Fields, D.E., Sampa, M.H. and Silva, B. (1996). *Estimates of Cancer Mortality Due to the Ingestion of Mineral Spring Waters from a Highly Natural Radioactive Region of Brazil*. Journal of Environmental Radioactivity, 33 (3), 319-329.
- Kaufman, A. and Libby, W., (1954). *Natural distribution of tritium*. Phys. Rev. 93, 337-1344.
- Kim, G., Dulaiova, H., Burnett, W.C., Swarzenski, P.W., Moore, W.S. (2001). *Measurement of ²²⁴Ra and ²²⁶Ra activities in natural waters using a radon-in-air monitor*. Environmental Science and Technology, 35, 4680.
- Langguth, H.R. (1966). Die Grundwasserverhältnisse Bereich des Velberter Sattels, Rheinisches Schiefergebirge, Der Minister für Ernährung. Landwirtschaft und Forsten, NRW, Düsseldorf.
- Lieser, K.H. (2001). *Nuclear and Radiochemistry*. 2nd edition. Germany: Wiley-VCH.
- Lloyd, J.W. and Heathcoat, J.A. (1985): *Natural inorganic chemistry in relation to groundwater*. Clarendon Press, Oxford.
- Martin, P., & Akber, R.A. (1999). *Radium isotopes as indicators of adsorption-desorption interactions and barite formation in groundwater*. Journal of Environmental Radioactivity, 46, 271-286.
- Milanovic, P.T. (1981): *Karst hydrogeology*. Water Resources Publications.
- Ministry of Environmental Affairs (1998): *Water resources in the West Bank*.
http://www.mena.gov.ps/part3/40_m.htm, (19.11.2008)

- Minster, T., Ilani, S., Kronfeld, J., Even, O. and Godfrey-Smith, D.I. (2004). ***Radium Contamination in the Nizzana-1 Water Well, Negev Desert, Israel.*** Journal of Environmental Radioactivity, 71, 261-273.
- Moon, D.S., Burnett, W.C., Nour, S., Horwitz, P., Bond, A. (2003). ***Preconcentration of radium isotopes from natural waters using MnO₂ Resin.*** Applied Radiation and Isotopes, 59, 255-262.
- Moore, W.S., Shaw, T.J., (1998). ***Chemical signals from submarine fluid advection onto the continental shelf.*** Journal of Geophysical Research, 103 (C10), 21543-21552.
- Moore, W.S., (2008). ***Fifteen years of experience in measuring ²²⁴Ra and ²²³Ra by delayed-coincidence counting.*** Marine Chemistry 109, 188-197.
- National Council on Radiation Protection and Measurements (NCRP). (1987). ***Ionization Radiation Exposure of the Population of the United States.*** Report No.93. National Council on Radiation Protection and Measurements, Bethesda, Maryland.
- National Council on Radiation Protection and Measurements (NCRP). (1994). ***Exposure of the Population in the United States and Canada from Natural Background Radiation.*** Report No. 94. National Council on Radiation Protection and Measurements, Bethesda, Maryland.
- ***Natural Radiation, Human Sources.*** Jefferson Lab.

http://www.jlab.org/div_dept/train/rad_guide/sources.htm/ (8/06/2009)
- Oliveira, J., Mazzilli, B., Oliveira, M., Silva, B. (1998). ***Seasonal variations of ²²⁶Ra and ²²²Rn in mineral spring waters of Aguas da Prata , Brazil.*** Applied Radiation and Isotopes, 49, 423-427.
- Palestinian Central Bureau of Statistics (PCBS). (2007)

<http://www.pcbs.gov.ps/census2007/default.aspx?lang=ar-jo> (4/09/2009)
- Palestinian Central Bureau of Statistics Press Release in the Occasion of the World Water Day ***“Coping With Water Scarcity”*** Which encounter in March 22, 2007.

http://www.pcbs.gov.ps/Portals/_pcbs/PressRelease/WaterPress07E.pdf (4/9/2009)
- Palestinian Water Authority (PWA). (2004). ***Historic Well Abstraction and Spring Discharge Database.*** West Bank: Palestine.

- Piper, A.M. (1944). *Graphical procedure in geochemical interpretation of water analysis*. Trans-American Geophysical Union, 25, 914-928.
- Porcelli, D. and Swarzenski, P.W. (2003). *The behavior of U- and Th-series nuclides in groundwater*. In: Bourdon, B., Henderson, G.M., Lundstrom, C.C., and Turner, S.P., (eds.), Uranium-series Geochemistry. Review in Mineralogy and Geochemistry, v.52, Geochemical Society and Mineralogical Society of Americapp.317-361.
- Rama & Moore W. S. (1984). *Mechanism of transport of U-Th series radioisotopes from solids into ground water*. Geochimica et Cosmochimica Acta, 48, 395-399.
- Roeffy and Raffety (1963). *Jerusalem District water supply, Geological and Hydrological Report*, Hashemite Kingdom of Jordan Central Authority. (unpublished).
- Roeffy and Raffety (1965). *Nablus District water resources survey, Geological and Hydrological Report*, Hashemite Kingdom of Jordan Central Authority. (unpublished).
- Scarpa, David (2002). *Capacity Building for a program in Water Resources Management in Gaza and the West bank*. Course1. Groundwater flow and Transport. Bethlehem University, 10–16.
- Singh, J., Singh, H., Singh, S., and Bajwa, B.S. (2008). *Estimation of Uranium and Radon concentration in some drinking water samples*. Radiation Measurements, Volume 43, Supplement 1, S523 –S526.
- Skeppström, K., & Olofsson, B. (2006). *A prediction method for radon in groundwater using GIS and multivariate statistics*. Science of the Total Environment, 367, 666-680.
- Spizzico, M. (2005). *Radium and radon content in the carbonate-rock aquifer of the southern Italian region of Apulia*. Hydrogeology journal, 13, 493-505.
- Sturchio, N. C., Banner, J. L., Binz, C.M., L.B. and Musgrove, M. (2001). *Radium geochemistry of ground waters in Paleozoic carbonate aquifers, midcontinent, USA*. Applied Geochemistry, 16, 109-122.
- Todd, D. (1980): *Ground water*, Prentice Hall Inc., London.
- United States Geological Survey (USGS). (2000) *Naturally Occurring Radionuclides in the Groundwater of Southeastern Pennsylvania*. USA.
- UNSCEAR 1982. *Ionizing radiation; sources and biological effects*. 1982 Report to the General Assembly, United Nations, New York.

- Vengosh, Avner. (2006). *Rooting Out Radioactive Groundwater*. Geotimes.
http://www.geotimes.org/may06/feature_RadioactiveWater.html (21/10/2008)
- Vengosh, A., Hirschfeld, D., Vinson, D., Dwyer, G., Raanan, H., Rimawi, O., Al-Zoubi, A., Akkawi, E., Ganor, J., Marie, A. (2008). **High Naturally Occurring Radioactivity in Groundwater in the Middle East: A New Challenge for Water Management**. (Unpublished)
- Webster, I.T., Hancock, G.J. and Murray, A.S. (1995). *Modelling the effect of salinity on radium desorption from sediments*. *Geochemica et Cosmochimica Acta*, 59(12), 2469-2476.
- World Health Organization (WHO). (2003). *Guidelines for Drinking Water Quality: Radiological Quality of Drinking- Water*. 3rd ed. Geneva, Switzerland.
- Zuckin, J.G., Hammond, D.E., Ku, T.L., Elders, W.A. (1987). *Uranium-Thorium series isotopes in brines and reservoir rocks from two deep geothermal boreholes in the Salton Sea geothermal field, Southeastern California*. *Geochimica et Cosmochimica Acta*, 51, 1719-1731.

APPENDIX I

²²⁶Ra concentration calculations in the studied wells

Sample	Incubation Time (days)	% of Sec Equilibrium	Cycle ID	Rn-222 CPM	2-sigma error	MEAN CPM / SD	blank CPM	sample-blank	Equil .Corr CPM	System Efficiency	corr DPM	Sample Vol. (L)	DPM / (L)	Pci/ L	Bq/L	
Izzariya (1)	31.11	0.9963	2	6.7	1.53	6.16	0.2	5.9643	5.99	0.07176	83.4	50	1.67	0.752	0.0278	
			3	5.2	1.37	0.7								0.19	0.086	0.0032
			4	6.63	1.53	11%										
			5	5.2	1.37											
			6	6.92	1.55											
			7	6.14	1.48											
			8	6.36	1.5											
Izzariya (1)	27.96	0.9935	2	6.52	1.52	5.97	0.24	5.734	5.77	0.07176	80.4	50	1.61	0.725	0.0268	
			3	5.96	1.46	0.33								0.09	0.04	0.0015
			4	5.67	1.43	6%										
			5	5.97	1.47											
			6	5.75	1.44											
JWC (4)	24.88	0.9886	2	1.21	0.75	1.42	0.19	1.234	1.25	0.07176	17.4	25	0.7	0.313	0.0116	
			3	1.71	0.85	0.23								0.11	0.051	0.0019
			4	1.64	0.84	16%										
			5	1.28	0.76											
			6	1.28	0.78											

²²⁶Ra concentration calculations in the studied wells

Sample	Incubation Time (days)	% of Sec Equilibrium	Cycle ID	Rn-222 CPM	2-sigma error	MEAN CPM / SD	blank CPM	sample-blank	Equil .Corr CPM	System Efficiency	corr DPM	Sample Vol. (L)	DPM / (L)	Pci/ L	Bq/L		
Herodion 2	25.02	0.9889	2	5.53	1.41	5.14	0.09	5.048	5.1	0.07176	71.1	50	1.42	0.641	0.0237		
			3	4.44	1.28	0.55								0.15	0.068	0.0025	
			4	4.81	1.35	11%											
			5	5.1	1.36												
			6	5.81	1.44												
Herodion (1)	30.89	0.9962	2	1.71	0.86	1.44	0.18	1.26	1.26	0.07176	17.6	34	0.52	0.234	0.0086		
			3	1.35	0.78	0.22								0.08	0.035	0.0013	
			4	1.43	0.8	15%											
			5	1.14	0.73												
			6	1.57	0.83												
PWA 1	31.03	0.9962	2	1.42	0.79	1.62	0.11	1.512	1.52	0.07176	21.1	34	0.62	0.28	0.0104		
			3	1.64	0.84	0.2								0.08	0.034	0.0013	
			4	1.42	0.79	12%											
			5	1.85	0.88												
			6	1.78	0.87												
PWA 11	30.92	0.9962	2	1.35	0.78	1.51	0.18	1.33	1.34	0.07176	18.6	26.5	0.7	0.316	0.0117		
			3	1.64	0.84	0.48								0.22	0.1	0.0037	
			4	1.21	0.75	32%											
			5	2.28	0.96												

²²⁶Ra concentration calculations in the studied wells

Sample	Incubation Time (days)	% of Sec Equilibrium	Cycle ID	Rn-222 CPM	2-sigma error	MEAN CPM / SD	blank CPM	sample-blank	Equil .Corr CPM	System Efficiency	corr DPM	Sample Vol. (L)	DPM / (L)	Pci/ L	Bq/L
PWA 11			6	1.07	0.71										
Izzariya (3)	31.96	0.9968	2	4.63	1.3	5.71	0.25	5.458	5.48	0.07176	76.3	34	2.24	1.011	0.0374
			3	5.99	1.46	0.8							0.31	0.141	0.0052
			4	5.35	1.39	14%									
			5	5.78	1.43										
			6	6.79	1.55										
Herodion (3)	28.97	0.9946	2	1.28	0.76	0.88	0.02	0.858	0.86	0.07176	12	50	0.24	0.108	0.004
			3	1	0.69	0.28							0.08	0.034	0.0013
			4	0.85	0.66	31%									
			5	0.59	1.43										
			6	0.67	1.55										
Herodion (3)	33.01	0.9974	2	0.78	0.64	0.9	0.07	0.826	0.83	0.07176	11.5	50	0.23	0.104	0.0038
			3	0.85	0.66	0.19							0.05	0.022	0.0008
			4	1.21	0.75	22%									
			5	0.71	0.61										
			6	0.93	0.67										

²²⁶Ra concentration calculations in the studied wells

Sample	Incubation Time (days)	% of Sec Equilibrium	Cycle ID	Rn-222 CPM	2-sigma error	MEAN CPM / SD	blank CPM	sample-blank	Equil .Corr CPM	System Efficiency	corr DPM	Sample Vol. (L)	DPM / (L)	Pci/ L	Bq/L
Asamoua			4	1.99	0.84	11%									0.0077
			5	2.06	0.76										0.0008
			6	1.57	0.78										
Izzariya (2)	27	0.9923	2	4.41	1.27	4.03	0.33	3.702	3.73	0.07176	52	50	1.04	0.468	0.0173
			3	3.99	1.22	0.37							0.1	0.043	0.0016
			4	3.49	1.15	9%									
			5	4.35	1.27										
			6	3.92	1.21										
Hundaza	31.88	0.9968	2	4.34	1.26	4.13	0.53	3.602	3.61	0.07176	50.4	50	1.01	0.454	0.0168
			3	3.49	1.15	0.41							0.1	0.045	0.0017
			4	3.99	1.23	10%									
			5	4.56	1.29										
			6	4.28	1.26										
Al - Rehea	32.01	0.9969	2	7.63	1.62	8.02	0.89	7.132	7.15	0.07176	99.7	50	1.99	0.898	0.0332
			3	8.56	1.71	0.57							0.14	0.063	0.0023
			4	7.71	1.64	7%									
			5	8.71	1.73										
			6	7.5	1.63										

²²⁶Ra concentration calculations in the studied wells

Sample	Incubation Time (days)	% of Sec Equilibrium	Cycle ID	Rn-222 CPM	2-sigma error	MEAN CPM / SD	blank CPM	sample-blank	Equil .Corr CPM	System Efficiency	corr DPM	Sample Vol. (L)	DPM / (L)	Pci/ L	Bq/L
Herodion 4	33.03	0.9974	2	3.71	1.18	3.38	0.46	2.92	2.93	0.07176	40.8	50	0.82	0.368	0.0136
			3	3.64	1.17	0.39							0.09	0.042	0.0016
			4	2.92	1.07	12%									
			5	3.64	1.17										
			6	2.99	1.08										

²²²Rn concentration calculations in the studied wells

Well Sample	protocol	Time of decay (day)	EXP(-λt)	Cycles	Rn-222 (pCi)	2-sigma error pCi	MEAN (pCi) / SD	blank (pCi/L)	Equil. Corr. (pCi/L)	dpm/L	Bq/L	Bq/m3
JWC4	Wat 250	0.1535	0.972564	1	244	69.2	225	0	231.3	513.59	8.56	8559.85
				2	229	67.3	66.65		32.6			
				3	179	60.5	29.62%		14.11%			
				4	248	69.6						
Herodion (3)	Wat 250	0.2618	0.953652	1	240	68.7	254.75	4.77	262.1	581.93	9.70	9698.78
				2	290	74.6	70.4		25.1			
				3	252	70.1	27.63%		9.57%			
				4	237	68.2						
Herodion 2	Wat 250	3.9840	0.485695	1	137	54.1	153.25	3.79	307.7	683.15	11.39	11385.78
				2	138	54.4	56.7		38.8			
				3	161	58	37.00%		12.61%			
				4	177	60.3						
Herodion (1)	Wat 250	1.1007	0.819124	1	160	57.7	156	6.67	182.3	404.72	6.75	6745.27
				2	157	57.4	57.175		5.0			
				3	157	57.4	36.65%		2.72%			
				4	150	56.2						

²²²Rn concentration calculations in the studied wells

Well Sample	protocol	Time of decay (day)	EXP(-λt)	Cycles	Rn-222 (pCi)	2-sigma error pCi	MEAN (pCi) / SD	blank (pCi/L)	Equil. Corr. (pCi/L)	dpm/L	Bq/L	Bq/m3
Izzariya (3)	Wat 250	1.0007	0.834107	1	263	71.5	260.5	17.2	502.7	1115.99	18.60	18599.90
				2	235	68.5	71.475		37.3			
				3	262	71.8	27.44%		7.42%			
				4	282	74.1						
PWA (11)	Wat 250	4.0035	0.483987	1	110	71.5	114.75	17.2	201.6	447.45	7.46	7457.54
				2	95.9	68.5	71.475		55.8			
				3	161	71.8	62.29%		27.70%			
				4	92.1	74.1						
PWA (1)	Wat 250	4.9778	0.405632	1	21.3	103	43.05	16.2	66.2	146.95	2.45	2449.14
				2	43.1	118	117		27.2			
				3	43.1	118	271.78%		41.16%			
				4	64.7	129						
Al Rehea	Wat 250	1.2500	0.797252	1	129	52.5	115.375	10.5	131.5	292.03	4.87	4867.19
				2	72.5	41.8	49.875		39.0			
				3	153	56.5	43.23%		29.65%			
				4	107	48.7						

²²²Rn concentration calculations in the studied wells

Well Sample	protocol	Time of decay (day)	EXP(-λt)	Cycles	Rn-222 (pCi)	2-sigma error pCi	MEAN (pCi) / SD	blank (pCi/L)	Equil. Corr. (pCi/L)	dpm/L	Bq/L	Bq/m3
Izzariya (2)	Wat 250	0.8736	0.853545	1	149	55.9	170.75	9.53	188.9	419.32	6.99	6988.67
				2	187	61.6	59.2		21.3			
				3	160	57.7	34.67%		11.30%			
				4	187	61.6						
Izzariya (1)	Wat 250	2.8458	0.596989	1	264	71.2	235.25	0	394.1	874.81	14.58	14580.25
				2	178	59.9	67.45		66.8			
				3	261	70.7	28.67%		16.96%			
				4	238	68						
Al Samou'	Wat 250	1.0792	0.822327	1	103	47.8	118.25	6.67	135.7	301.23	5.02	5020.46
				2	141	54.7	50.675		18.8			
				3	111	49.4	42.85%		13.83%			
				4	118	50.8						
Al Fawar	Wat 250	1.9625	0.700657	1	33.8	31.3	45.275	2.83	60.6	134.49	2.24	2241.42
				2	60.4	38.7	34.6		16.0			
				3	37.8	32.6	76.42%		26.47%			
				4	49.1	35.8						

²²²Rn concentration calculations in the studied wells

Well Sample	protocol	Time of decay (day)	EXP(-λ.t)	Cycles	Rn-222 (pCi)	2-sigma error pCi	MEAN (pCi) / SD	blank (pCi/L)	Equil. Corr. (pCi/L)	dpm/L	Bq/L	Bq/m3
Hundaza	Wat 250	1.9854	0.697752	1	141	54.4	138	5.71	189.6	420.90	7.01	7015.00
				2	138	54.4	54.075		36.6			
				3	104	48.3	39.18%		19.29%			
				4	169	59.2						